Detector environment and detector response : a survey

Holmstedt, Göran; Magnusson, Sven Erik; Thomas, Philip H

1987

LUND UNIVERSITY · SWEDEN
INSTITUTE OF SCIENCE AND TECHNOLOGY
DEPARTMENT OF FIRE SAFETY ENGINEERING
REPORT LUTVDG/(TVBB-3039)
ISSN 0282-3756

G. HOLMSTEDT - S.E. MAGNUSSON - P.H. THOMAS

DETECTOR ENVIRONMENT AND DETECTOR RESPONSE.
A Survey

LUND 1987

Holmstedt, G. - Magnusson, S. E. - Thomas, P. H.

DETECTOR ENVIRONMENT AND DETECTOR RESPONSE.
A Survey.

Lund December 1987

List of contents

MAIN LIST OF NOTATION

A	constant = $g/(c_p \ T_\infty \ \rho_\infty)$ (m^5/Js)
A_L	effective area of heat sensing element (m^2)
b	fire plume radius (m)
C_N	particle number concentration (cm^{-3})
c_p	specific heat (J/kg K)
D	optical density ($^{10}\log$ (100/T)) where T is transmission
D_L	optical density per unit length. If measured in dB/m the unit of D_L is called obscura (ob)
D_o	smoke potential, ob · m^3/g
D_p	particle diameter (μm)
h_c	convective heat transfer coefficient (W/m^2K)
H	room height or distance fire source - ceiling (m)
I	ionization detector chamber current (A)
I_o	base level of I (A)
K	plume equation constant
m_L	mass of sensing element (kg)
N	particle number concentration (cm^{-3})
Q	fire heat release rate (kW)
Q_c	convective part of Q (kW)
Q_f	fictitious heat release rate, derived from room ventilation (kW)
Q_n	heat from normal room heating (kW)
r	ceiling jet radius (m)
T	transmittance (%), temperature (K)
ΔT	temperature difference (K)
ΔT_g	change in gas temperature (K)
ΔT_L	change in sensing element temperature (K)
ΔT_m	maximum value of temperature change in ceiling jet (K)
ΔT_p	change in plume temperature (K)
ΔT_m^*	dimensionless form of ΔT_m
ΔT_2^*	dimensionless temperature change defined by Eq 3.11c
T_∞	ambient temperature (K)
t_2^*	dimensionless time, see Eq 3.11a

U	ceiling jet gas velocity (m/s)
U_m	maximum value of U over ceiling jet thickness (m/s)
U_m^*	dimensionless form of U_m
X	relative signal output from ionization detector
V	volume of room

Greek letters

α	fire growth constant (kW/m^2)
α_o	entrainment coefficient
α_c	recombination coefficient
α_s	particle size parameter
γ	fractional generation rate of CO
λ	wavelength (μm)
ρ_∞	ambient density (kg/m^3)
τ	time constant
τ_r	residence time

FOREWOORD

This manuscript forms the report of a Brandforsk project "Detection environment". The original objectives were stated as (Brandforsk PM 1982-03-01 P1/1982 ä 11:4)

- to identify, structure and summarize the problem
- to determine detail and art of environment variables to be studied
- to determine which geometric variables (room size, room shape and planning design) are important
- to find a form for publishing the results such that the results will be easily available to the detection industry
- to prepare for a possible continuation of the project

Due to staff capacity problems, the completion of the project has been severely delayed. Partly to compensate for this, the objectives of the investigation have been reformulated in the sense that the scope is considerably more ambitious and comprehensive. The main changes or additions are the following: detector characteristics have been described and detector output related to environmental variables, the possibility of more rational design methods, including use of standard test data, has been explored and approximate criteria derived for the fire to dominate ventilation and pre-fire heating.

The authors thank Prof Ove Pettersson for valuable comments and a careful review.

1 INTRODUCTION

Fire detection techniques have made great progress during the last decades. This evolution is partly based on increased knowledge regarding fire processes and fire signatures in general, partly on improvements in hardware design and in the processing and analysis of response signals. The present report makes an attempt to summarize some of these developments with an emphasis on fire physics and the detection environment, detector response and false alarms. Important areas omitted include design of signal carrying and transmitting system, detector tolerance for non-fire or non-aerosol environmental loading (corrosion, vibration, impact, etc), signal detection algorithms or software control in general of the electronic circuits.

2 FIRE SIGNATURES

A fire has many properties, any one or combination of which can be used to identify its presence. As soon as a material is heated certain changes occur which can be identified. However, most of the signatures that we will be discussing are associated with either the smouldering or ignition stage of a fire. Material property data from tests involving later stages of the burning process may have questionable relevance.

In sections 2.1 - 2.3 below will be given a fragmentary, short description of fire signatures. As the main area of the survey concerns smoke detector, section 2.4 will describe smoke aerosol characteristics in some more detail. Most of the material is based on the two publications by Benjamin /1/ and Lee and Mulholland /2/. In section 2.5, finally, some data are presented on aerosols in non-fire environments.

2.1 Aerosol Signatures

The process of combustion releases into the atomsphere both solid and liquid particles which range in size from about .01 to 10 micrometers. These particles, when suspended in air, are called aerosols. In general, the aerosol can be divided into those particles which are less than 0.3 micrometers and do not scatter light; and those which are larger than 0.3 micrometers and do scatter light and are therefore visible. The visible size particles are generally what we call smoke or products of combustion. The most frequent range of aerosol particle sizes are from 0.1 to about 2.0 micrometers; and the aerosol type detectors are designed to operate in this range. The fact that the particle size for the smouldering fire is generally considerably larger than that for the flaming fire and the size distribution of an aerosol will change significantly with time will be discussed below.

2.2 Energy Release

Another fire signature of importance is the energy release. The energy released is in the form of both light and thermal energy. The light band of energy includes both the visible, infrared and ultraviolet spectrum, and all of these are the basis for various types of detectors. The thermal energy forms a buoyant convective plume, which is also used to trigger various types of detectors. Reference 56 details rate of energy release process for some combustibles and fuel packages.

2.3 Gas Signatures

A fire will produce a wide range of chemical products as gas, depending upon the nature of the material burning. One of the gases which is most common to all combustion is CO (carbon monoxide). Another signature which has been used is the presence of hydrocarbons, which are another product of the evolution from most fires.

2.4 Some Properties of Smoke Aerosols Pertinent to Smoke Detector Technology

Rational smoke detector design technology should be based on a knowledge of the characteristics of the smoke in terms of the attributes sensed by the detector; i.e. particle size distribution, number concentration, mass concentration and refractive index. The data presented is mostly taken from standard test procedures, where approval or sensitivity criteria often are expressed in terms of the optical density or the light obscuration of the smoke surrounding the detector. When measuring the optical density, the light source will in most cases have a wavelength corresponding to white light and the photocell a sensitivity corresponding to the human eye. In order to establish the relation between detector output and optical density measurements the latter must be linked to the mentioned aerosol properties.

2.4.1 Initial Particle Size Distribution

In Euronorm EN54 part 9, the sensitivity test, detectors are exposed to a number of fires, selected to produce the whole range of particle size, shape, concentration and material expected by the different kinds of real fires. Fig 2.1 shows two examples of the size distribution investigated /3/, the flaming wood fire and the smouldering wood fire. These represent two extreme cases of particle size. Other test fires (polyurethane, heptane, glowing wick) have size distributions in between.

Ing fig 2.1, the quantity ΔC_N represents the number of smoke particles in the particle size range $\log D_p$ to $\log D_p + \Delta(\log D_p)$. The Δ representation is used because experimental data was obtained as average number of particles within certain discrete ranges. The logarithmic representation is chosen in order to compress data.

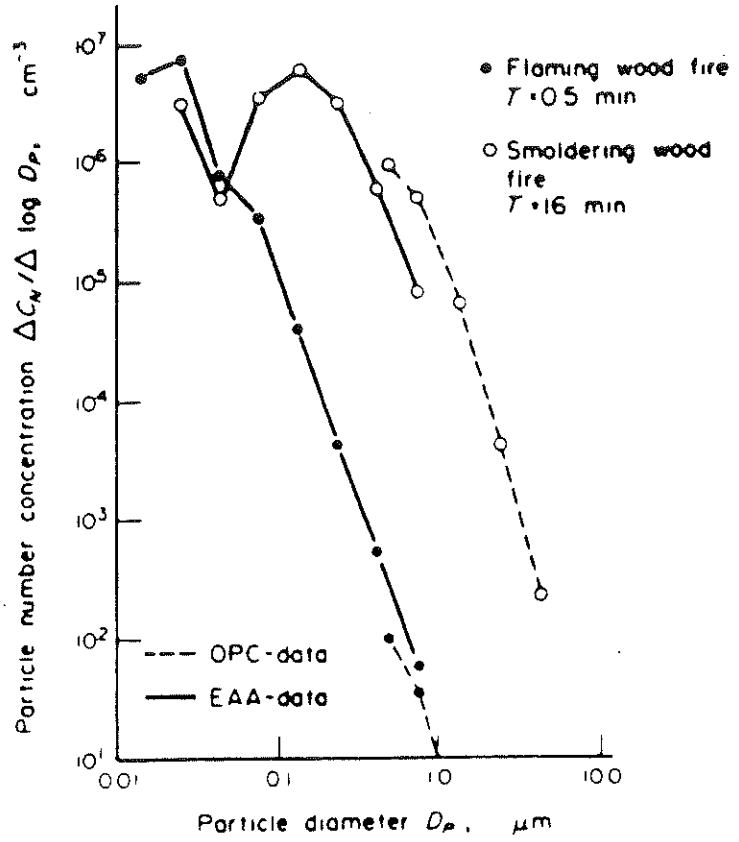

Fig 2.1 Examples of the particle number distribution of two test fires /3/

2.4.2 Mass Concentration and Optical Density

Lee and Mulholland /2/ measured the properties of smouldering lamp wick smokes and heptane black soot smoke in the UL 217 Standard evaluation chamber. Particle size distributions are shown in Fig 2.2 and the relation between measured optical density per meter and mass concentration in mg/m^3 is shown in fig 2.3.

The ratio of optical density per meter to mass concentration is termed particulate optical density (POD) and is shown to be relatively constant property for each of the two modes of burning. It had earlier been reported by Seader and Einhorn /4/ that experiments with the NBS smoke density chamber and a number of combustibles revealed the same relationship for much higher smoke concentration, cf Figs 5.16 and 5.17 in section 5.4.2.2. It thus appears that for white light

$$POD = 3400 \text{ kg/m}^2 \text{ (flaming combustion)} \quad (2.1a)$$

$$POD = 1900 \text{ kg/m}^2 \text{ (non-flaming combustion)} \quad (2.1b)$$

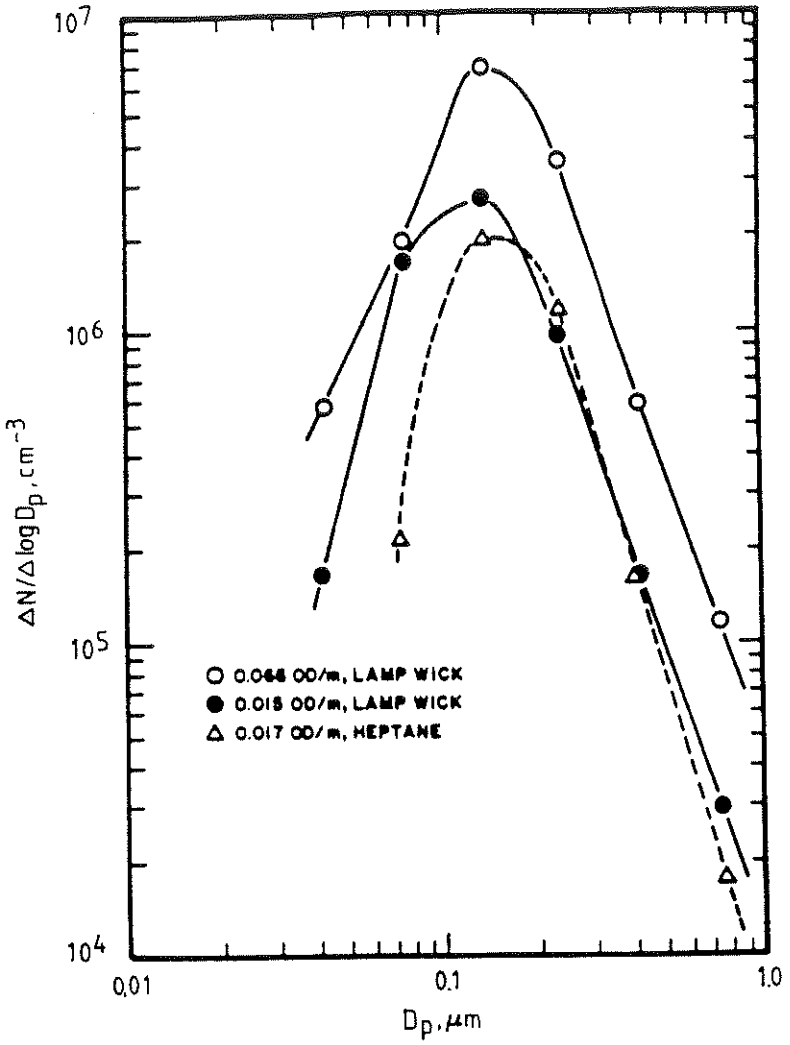

Fig 2.2 Particle size distribution for lamp wick and heptane smokes /2/. N denotes number of particles per cm^3 (= C_N in fig 2.1)

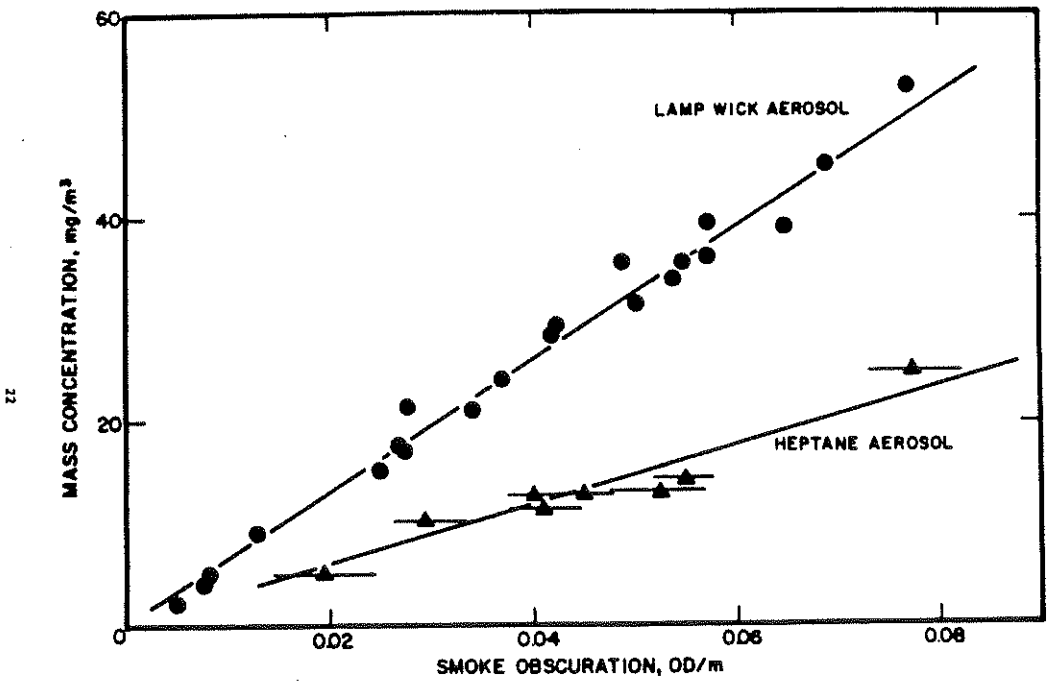

Fig 2.3 Mass concentration versus smoke obscuration (optical density per m) in UL 217. (Bars represent shift of obscuration during measurement) /2/

There does not seem to be any data confirming the relationships above for exposure conditions outside those reported in /2/ and /4/. The constancy of the quantity POD is theoretically explained in section 5.4.2.

2.4.3 Number Concentrations, Particle Sizes and Coagulation

Particle coagulation (ageing) due to Brownian collisions plays an important role in changing the size distribution of an aerosol. Coagulation is said to occur when two particles collide and form a single particle whose volume is the sum of the volumes of the original two particles. The number of particles is thereby decreased by one while the total volume of the particles remains the same.

The fundamental quantity for coagulation is the coagulation coefficient, τ, which is defined by

$$\frac{dN}{dt} = -\tau N^2 \qquad (2.2)$$

The fact that the loss rate is proportional to the square of the number concentration explains the fact that the rate of particle loss is much faster at higher concentrations. An illustration is given by Fig 2.4 /2/.

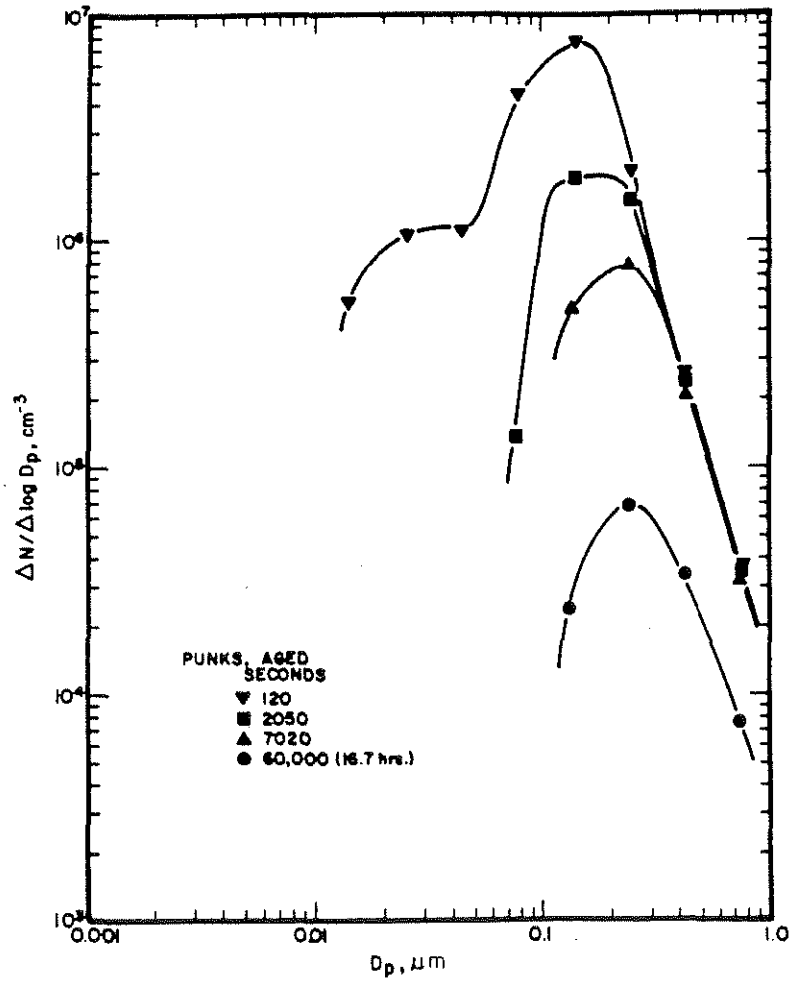

Fig 2.4 Aging of punk aerosol up to 16 hours /2/

The data shows a variation of two orders of magnitude in the total number of particles/cm^3 over a 16-hour period. Almost the whole coagulation process is limited to aerosol particles with $D_p < 0.1 - 0.2\ \mu$. The material in Fig 2.4 was punk. An analysis was also made for the standard test fuels smouldering lamp wick and heptane. Fig 2.5 shows the concentration as a function of smoke obscuration for aerosols of different initial concentrations.

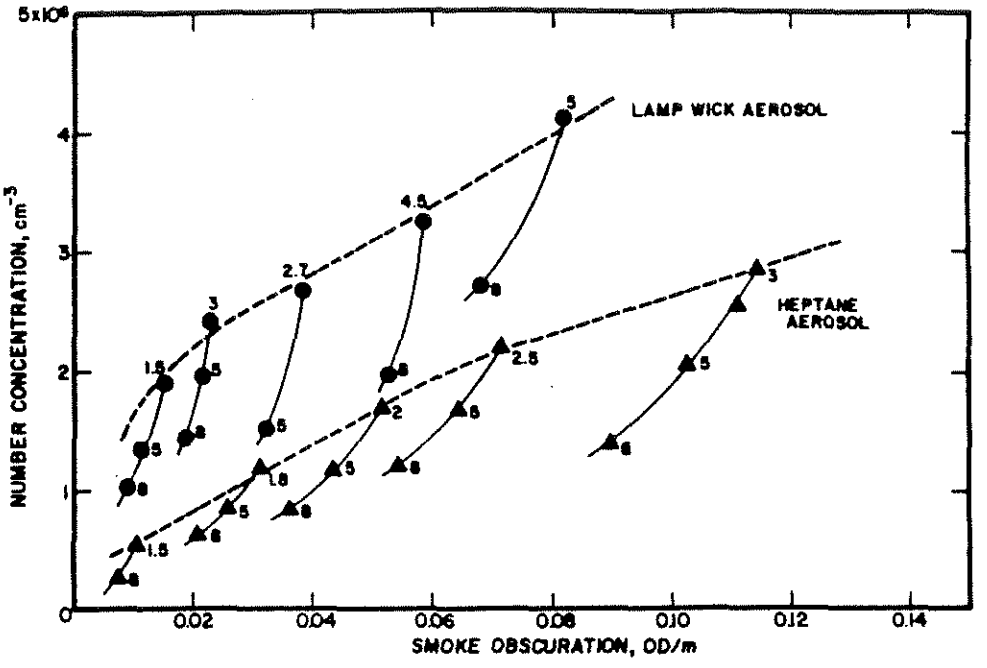

Fig 2.5 Number concentration versus smoke obscuration in UL 217 (The numbers indicate age in minutes) /2/

Numbers adjacent to the data points denote the age of the aerosols, measured from the time the burning specimen was inserted into the chamber to the time the aerosol was sampled by the monitor. Numbers at the top of the curve also indicate the minimum time for generation to reach the indicated levels.

The analysis of a given aerosol as it aged are connected by the short curves. From these curves it can be shown that the light obscuration per particle increases with aging. For example, obscuration of lamp wick aerosols with almost identical concentration, 2.6×10^6 cm^{-3}, was about 0.04 OD/m for a 2.7-minute aerosol, but over 0.07 OD/m for an 8-minute aerosol. Consequently, there is no linear relationship between optical density and number concentration such as the one exhibited in Fig 2.3 between optical density and mass concentration. The effect of the coagulation process and detector output will be discussed in section 5.4.

2.4.4 Smoke Production

We will start this section by repeating some basic definitions of smoke measurement

D = optical density denotes attenuation of light by smoke and is defined by

$$D = \log \left(\frac{100}{T}\right)$$

where T = transmittance in percent. D_L denotes light attenuation per length L and is measured in dB/m (also called obscura (ob)).

$$D_L = 10\ D/L = 10 \log \left(\frac{100}{T}\right) \text{ dB/m}$$

If the mass W gm is burnt in a volume of V m^3 and the measured optical density/m = D/L then D_o is defined by

$$D_o = 10 \frac{D}{L} \frac{V}{W} \text{ (dB/m)} \cdot m^3/g = \text{ob} \cdot m^3/g$$

As defined, 1 ob corresponds to a smoke concentration giving an attenuation of 1 dB/m, which in turn roughly corresponds to a visibility of 10 m. /5/. In Figs 2.3 and 2.5, the unit OD/m corresponds to 10 ob.

Rasbash and Pratt consider in /5/ some of the major difficulties that confront the estimation of smoke produced by fires. They include the confusion over the units in which smoke is expressed, reliability of laboratory test methods for smoke production developed so far, and the factors which may cause a difference between laboratory tests on the one hand and fire tests in general, and fire ground conditions on the other. Also, a number of approximate working formulae were developed to estimate D_o of materials burned in fire tests, from measurements of smokiness, D_L, obtained in the test, together with other data, such as gas analysis or temperature, that may be available. On the whole, values of D_o obtained in this way did not differ radically from values obtained under flaming conditions using bench tests, but there is evidence that under ventilation-controlled conditions with vertical vents, substantially higer values of D_o may be obtained than under fuel-controlled conditions. From information on D_o thus obtained, combined with information on D_o available from bench tests, a tentative list of values of D_o was given, for different materials burning under different conditions, which may be used as a first step towards predicting smoke output and smokiness in fire situations. See Table 2.1. (P_L is the fraction of fuel converted to volatiles).

TABLE 2.1

Recommended values of smoke potential (D_o) of different combustible materials under conditions of flaming combustion /5/

		D_o (ob m^3/g)
P_L > 75% (assume P_L = 100)		
Fibreboard burning freely at a vertical surface		0.1
Wood, plywood (fuel controlled free burning)		0.15
Wood (ventilation controlled burning; vertical vents)		0.6
Hardboard		0.3
Flexible polyurethane foam		0.9
Flexible polyurethane foam (ventilation controlled burning; vertical vents)		1.5
Nylon		1.8
Polyethylene		1.8
Polyethylene foams		3
Polystyrene (in free use, i.e. not stuck to walls and ceiling)		7
Petrol		3
Kerosene and fuel oil		5
Foam rubber		4.5
P_L < 75%		
Rigid PVC sheets	(P_L=60%)	2
ABS	(P_L=75%)	4
Rigid polyurethane foam	(P_L=60%)	3
Glass reinforced polyester	(P_L=75%)	0.8
Fire retardant GRP	(P_L=50%)	2
Polypropylene	(P_L=75%)	2
Linoleum	(P_L=60%)	1
Plasterboard	(P_L=18%)	0.05
Chipboard	(P_L=75%)	0.4
Phenol formaldehyde foam	(P_L=75%)	4

2.5 Some Data on Aerosols in Non-Fire Environments

Fragmentary aerosol data on non-fire environments are presented below.

2.5.1 Concentration Range

A schematic summary is presented in Table 2.2 /6/ which gives approximate concentration ranges (in mg/m^3) measured outdoors and indoors from tobacco smoke, dusts, aerosols from cooking, welding, spraying processes etc.

Recalling that a concentration of 30 mg/m^3 corresponds to the optical density 1 dB/m or 1 ob, (using a POD-value of 3300 m^2/kg) many activities lead to particle concentrations exceeding the actuation threshold.

2.5.2 Dwellings

In /7/ particle size distributions in 11 different dwellings was studied 5-7 days. Fig 2.6 gives the daily variation of

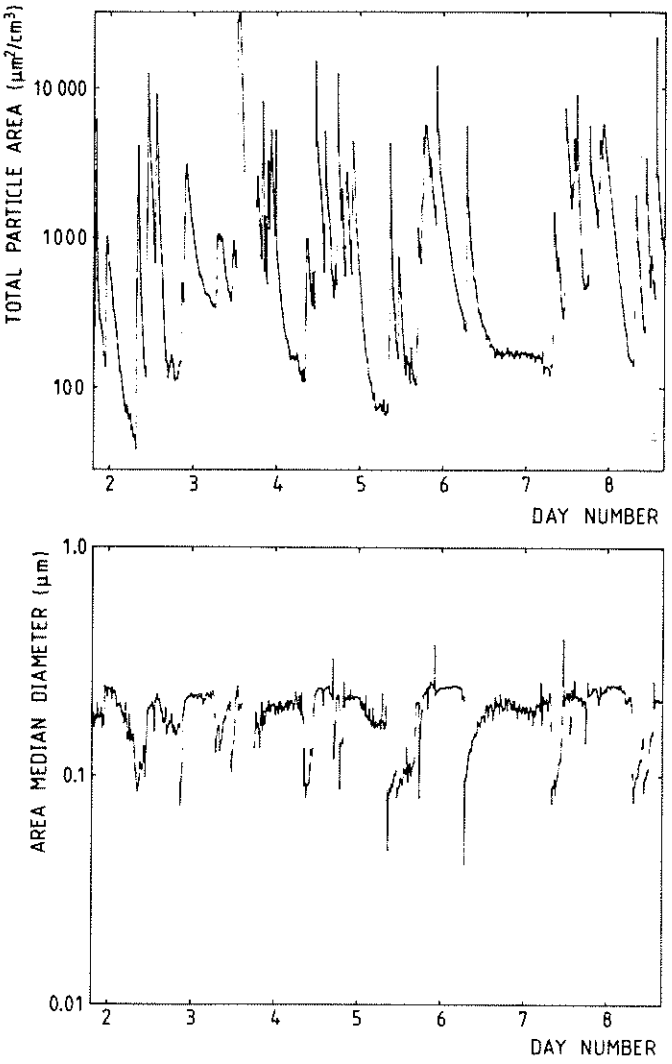

Fig 2.6 Measured variation of total particle area and mean area diameter for a dwelling /7/

Table 2.2

Approximate particle concentration ranges (mg/m^3)

Indoors		Outdoors	
Activity, equipment etc	conc. mg/m^3	Activity, equipmment etc	conc. mg/m^3
Smoke plume from coal power plant	$8x10^3$	Exhaust system grinding	$5x10^2$
		Exhaust system welding	$4x10^2$
Waste incineration	$2x10^3$	Oil fog	$1.5x10^2$
		Foundary	10^2
Oil firing	$2x10^2$	Dust from granulator	$5x10^1$
Oil burner	1,5x10	Welding, limited ventilation	10
Industrial areas			
very dirty	5.0	Welding, good venti-	
dirty	2.0	lation	1
normal	1.0		
		Hospital, HEPA-	
Big city	$5x10^{-1}$	filtered air	10^{-2}

total particle area and mean area diameter for a dwelling with frequent *cooking* and *smoking*. Using an average material density of 1.5 g/cm^3 and mean diameter = 0.2 μm, even the highest measured value of particle area = 20 000 $(\mu m^2)/cm^3$ corresponds to optical density 3 x 10^{-3} ob, far too small to cause a false alarm.

Remark. Non-fire aerosols is an area where much more extensive and specified data should be available and where continued efforts to collect and analyze data should be considered.

3 TRANSPORT OF HEAT AND COMBUSTION PRODUCTS

3.1. Fire As a Signal

Detectors detect signals and a fire detector detects some emission from a fire. Thermal radiation is independent of the flow of gases but heat gaseous emission and particulate matter are not. They are carried by the thermally driven plume which becomes established above the fire, provided there is no interference by other air currents.

Heat sources present in an enclosure before the fire will have established a flow pattern which is also affected by the ventilation and in some buildings by the external wind, the effect of which can be transmitted through the building envelope. These together are the "noise" against which the fire has to be detected and they determine, to an order of magnitude, the size of fire which can be distinguished from the background. It is a property of the enclosure design, the heating and ventilation systems etc.

By and large, for rooms ventilated for human occupation, with say 5 air changes or fewer per hour (i.e. a residence time of 720 sec), the ventilation should have little or no effect on the thermal plume. For a room 3 m in size, the mean air movement is about 3/720 m/sec which is far less than in a thermal plume, which at 10^{o}C above ambient will move 1/2-1 m/s.

Ventilation in "clean" rooms and heating are other matters. In well insulated property the background heating for comfort will be less than where the room insulation is poor and detection should be easier since the fire must produce flow velocities (and momenta) at least comparable in magnitude with those of the background heating for reliable detection by any method dependent on air movement. For the sake of generality and its relevance to highly ventilated "clean" rooms we shall however include ventilation in our very crude considerations in 3.3.

The preceeding section 3.2 will summarize the plume and ceiling jet equations for the case when the convective flow from the fire clearly dominates air movements from normal heating and ventilation. These equations form the base for the design process outlined in chapter 7.

3.2 The Fire Dominated, Buoyancy-Induced Flow

3.2.1 Formulas for Plumes and the Turning Region

In fires, fuel exothermally combines with oxygen to form hot, low density combustion products. To maintain this process, air surrounding the fire is drawn into the combustion region, creating an upward moving turbulent plume. Due to the low density of the plume, more air is entrained either to react

with unburned pyrolyzates or to simply dilute the plume. When the plume hits the ceiling, it turns to flow along the ceiling in an axisymmetric pattern. Fig 3.1 /8/ shows schematically the geometry, and other characteristics of the plume, turning region and ceiling flow. In figure 3.1 U denotes vertical velocity, b effective half width, h ceiling jet thickness, δ thickness of viscous sublayer, F_1 friction factor.

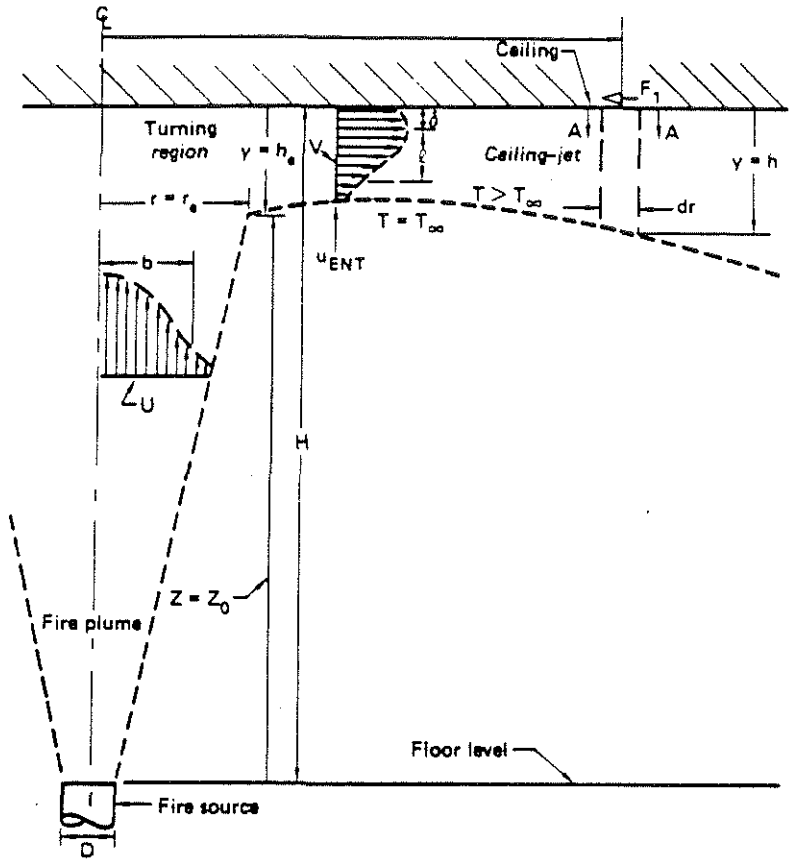

Fig 3.1 Schematic of idealized fire plume /8/

The thermal plume above fire source depicted in Fig 3.1 has been studied extensively. The width, velocity and temperature of the plume are functionally dependent on fire heat release rate and height above the fuel source in the following manner:

plume radius $b \sim Z$ (3.1a)

centerline velocity $U \sim A^{1/3} Q_c^{1/3} Z^{-1/3}$ (3.1b)

centerline excess temperature $\Delta T \sim A^{2/3} [T_\infty/g] \cdot Q_c^{2/3} Z^{-5/3}$ (3.1c)

where

Z = height above (virtual) fire source
Q_c = convective heat release
A = $g/c_p\ T_\infty\ \rho_\infty$
c_p = air heat capacity
T_∞ = ambient temperature
ρ_∞ = ambient density

As discussed later, these equations will be relevant for calculation of activation time of detection inside the turning region of Fig 3.1. We will first turn our attention to the ceiling jet region of the same figure.

3.2.2 Ceiling Jet Equations

3.2.2.1 Steady State - Growing Fires

The plume equations in section 3.2.1 are strictly valid only for steady state fires with a constant Q. For transient growing fires, two procedures are available in practice. In the first one, transport time from combustion region to the measurement point is neglected and temperature etc calculated as for steady state fires and based on the instantaneous value of Q. This is known as the quasi-steady approximation.

For the ceiling jet region, this simplification may be too coarse and the transient nature of the flow cannot be neglected. The problem then shifts to finding expressions for $Q = f(t)$ which are both amenable to analytical treatments and realistic descriptions of the actual fire growth process. Investigations have shown that algebraic expressions of the type

$$Q = \alpha\ t^p \qquad (3.2)$$

with $p = 2$ are acceptable approximation for a large class of fires. Appendix C of the NFPA 72E standard lists three fires which have t^2 type fire growth behavior. A slow developing fire is defined as one which would take 600 seconds from the time of flaming ignition until it reaches a heat release rate of 1055 kW (1000 BTU/s). A medium growth rate fire reaches the same heat release rate approximately 300 seconds after flaming ignition occurs. The fast developing fire requires 150 seconds to reach a heat release rate of 1055 kW . In addition, a fourth t^2 fire has been developed in /9/. This fire has been defined as one which takes 75 seconds to reach a heat release rate of 1055 kW . These four fire growth curves are plotted in Figure 3.2, taken from /9/. The corresponding value of α are 0.0029, 0.0117, 0.0469 and 0.1876 (kW/s^2), respectively.

Until more experimental validation is available, the curves in fig 3.2 should be used with caution in practical design.

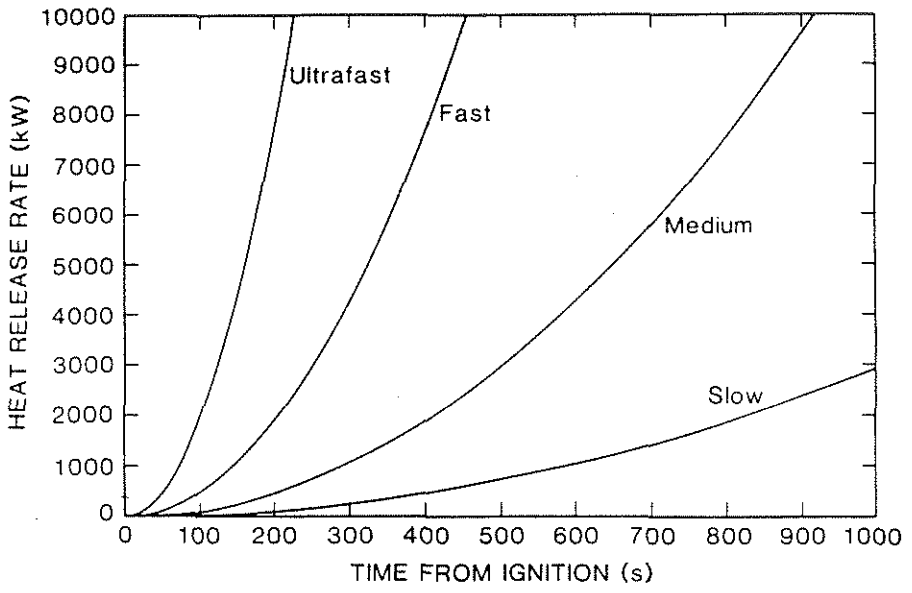

Fig 3.2 Plot of t^2 fire growth curves /9/

The inaccuracy in using the quasi-steady approximation changes with location. Velocities in fire plume and ceiling jet are of the magnitude 1-5 m/s. Thus the error introduced may be only a few seconds for locations close to the fire but some ten seconds for a more distant region.

3.2.2.2 Quasi-Steady Approximation for Ceiling Jet

Correlations of ceiling-jet temperatures and velocities from experiments using steady fire sources have been published by Alpert /15/. In metric form they are:

$$\Delta T_m = 16.9\ Q^{2/3}/H^{5/3} \qquad \text{for } r/H < 0.18 \qquad (3.3a)$$

$$U_m = 0.95\ (Q/H)^{1/3} \qquad \text{for } r/H < 0.15 \qquad (3.3b)$$

$$\Delta T_m = 5.38\ (Q/r)^{2/3}/H \qquad \text{for } r/H > 0.18 \qquad (3.4a)$$

$$U_m = 0.2\ Q^{1/3}\ H^{1/2}/r^{5/6} \qquad \text{for } r/H > 0.15 \qquad (3.4b)$$

ΔT_m and U_m denote maximum values.

By defining a dimensionless maximum temperature rise

$$\Delta T_m^* = \Delta T_m\ (c_p^2\ \rho_\infty^2\ H^5/T_\infty\ Q_c^2)^{1/3} \qquad (3.5)$$

and dimensionless maximum velocity

$$U_m^* = U_m \, (c_p \, T_\infty \, \rho_\infty \, H/gQ_c)^{1/3} \qquad (3.6)$$

equations 3.3 - 3.4 may be replaced by

$$\Delta T_m^* = 6.18 \qquad \text{for } r/H < 0.18 \qquad (3.7a)$$

$$\Delta T_m^* = 1.97 \, (r/H)^{-2/3} \qquad \text{for } r/H > 0.18 \qquad (3.8a)$$

$$U_m^* = 3.16 \qquad \text{for } r/H < 0.15 \qquad (3.7b)$$

$$U_m^* = 0.65 \, (r/H)^{-5/6} \qquad \text{for } r/H > 0.15 \qquad (3.8b)$$

3.2.2.3 Fires Growing According to t^2: Ceiling Jet Expression

In order to avoid the quasi-steady assumption Heskestad /17/ proposed a generalization of the steady state functional dimensionless expressions to include time. From experiments he and Delichatsios /16/were able to derive correlations of maximum temperature rise and velocity for the unconfined ceiling jet flow and with fires growing according to the expression $Q = \alpha \, t^2$. Beyler /18/ reviewed these expressions and arrived at the slightly different equations given below

$$\Delta T_2^* = \begin{cases} 0, & t_2^* \leq (t_2^*)_f \\ \left[\dfrac{t_2^* - 0.954 \, (1 + r/H)}{0.188 + 0.313 \, r/H}\right]^{4/3}, & t_2^* > (t_2^*)_f \end{cases} \qquad (3.9)$$

$$U_2^* / \sqrt{\Delta T_2^*} = 0.59 \, (r/H)^{-0.63} \qquad (3.10)$$

where

$$t_2^* = t \, / \, [A^{-1/5} \, \alpha^{-1/5} \, H^{4/5}] \qquad (3.11a)$$

$$U_2^* = U \, / \, [A^{1/5} \, \alpha^{1/5} \, H^{1/5}] \qquad (3.11b)$$

$$\Delta T_2^* = \Delta T \, / \, [A^{2/5} (T_\infty/g) \, \alpha^{2/5} \, h^{-3/5}] \qquad (3.11c)$$

$$A = g \, / \, [c_p \, T_\infty \, \rho_\infty] \qquad (3.11d)$$

$$\alpha = Q \, / \, t^2 \qquad (3.11e)$$

$$(t_2^*)_f = 0.954 \, (1 + r/H) \qquad (3.11f)$$

ΔT_2^* and U_2^* denote maximum values within the ceiling layer and $(t_2^*)_f$ is the non-dimensional arrival time of the initial heat front.

The main difference between the expressions given above and the original ones are that the former have the correct behaviour in the quasi-steady limit.

Eqs 3.1 - 3.11 will form the basis for the design procedure described in chapter 7.

3.3 Approximate Criteria for Fire to Dominate Ventilation and Pre-Fire Heating

We shall consider two ventilation criteria, additional to the criterion that the fire should be thermally stronger than the background.

1. We assume the background heating and ventilation in a room produces a stratified hot gas layer and we seek to define the fire plume which can penetrate this.

2. Normal ventilation is designed to effect a certain circulation of air, defined by a residence time (or number of air changes per hour) and we shall compare this with a circulation time based on the size of the fire plume.

There are various systems of ventilation which have inlets and extract openings in different positions, some of which will interfere more and some less with a fire plume. Inlet at low level and extract at high level as in the "low momentum displacement system", might be expected to be more favourable to detection then the reverse or other combinations. What follows is therefore little more than an indication of how certain of the variable factors viz fire, ventilation rate, background heating and scale may exert influence for a given geometry, a given design of ventilation system and a given position of the fire etc.

Consider the penetration of a layer. A plume gains mass and its temperatures falls as it ascends. The momentum of unit mass in the plume is least near the ceiling, and we will characterize the penetrating capacity of the vertical plume by its properties at the ceiling.

3.3.1 Theory

We define Q the rate of energy release by the fire, viz the fire power

Q_n the rate of energy release by the normal heating

α_o the entrainment coefficient

ρ the plume density taken as equal to that of air
c the plume specific heat at constant pressure taken as that of air
T_∞ the ambient absolute temperature
h the heigt of the base of a hot layer of air or of combustion products above an effective point source
H the height of the enclosure
V its volume
and τ_r the residence time of the normal ventilation.

The volumetric flow of the ventilation is V/τ_r and if it was confined only to a small layer the effective volume and effective time would be reduced equally. The temperature rise of the pre-existant layer depends only on the flow rate

$$\overline{\Delta T}_1 \approx \frac{\dot{Q}_n \tau_r}{\rho c V} \qquad (3.12a)$$

but in the prescens of a fire $\overline{\Delta T}_1$ becomes

$$\overline{\Delta T}_1^1 \approx \frac{(Q + Q_n)\tau_r}{\rho c V} \qquad (3.12b)$$

whatever its thickness.

The mean plume temperature rise at the base of the layer is known from plume theory (see Eq 3.1c)

$$\overline{\Delta T}_p = \frac{1}{K} \frac{T_\infty}{gh} \left[\frac{g Q}{\rho c T_\infty h}\right]^{2/3} \qquad (3.13)$$

where K depends on the entrainment coefficient α_o. Zukoski's formulation of plume theory for a Gaussian profile gives

$$K = 3 \left[\frac{12\Pi\alpha_o^2}{25}\right]^{2/3} \qquad (3.14)$$

An approximate condition for the penetration of the thermal layer already in the enclosure may be stated as

$$\overline{\Delta T}_p > \overline{\Delta T}_1 \qquad (3.15)$$

But 'h' has an initial value. If the plume does not penetrate the layer then the plume will spread out beneath it and a second layer will build up between it and the fresh air beneath. As it deepens the height of the fresh air layer diluting the plume lessens and the plume temperature at the base of the layer rises. Eventually mixing must occur but perhaps only at a late stage when the concept of a stratified layer is inapplicable.

If one then argues that for detectors to respond one requires only that the fire is sufficiently more powerful than the normal background heating a nominally representative value of 'h' may be taken and a conservative choice for inequality (3.15) is to take H.

If there is no layer and the air in the enclosure is thoroughly mixed then no account need be taken of Q_n because the plume temperature is, in effect, an excess above ambient. On the other hand the worst condition for interference with the fire plume will probably be for a single heat source eg a convection heater. For N equal separate heat sources one could as a rough guide consider Q_n/N as a measure of the background heating interferring with the fire plume. Complete mixing is in effect equivalent to a large number of sources ($N \rightarrow \infty$) totalling Q_n and such a limit removes the effect of Q_n on the plume and is consistant with the remark above that the plume is above ambient. The degree of mixing is dependent on the arrangement of the ventilation inlets and extracts and the position and number of thermal sources making up the total of Q_n. Such assessments will require either analogue or numerical modelling.

If there is no layer and the ventilation is producing air currents that might interfere with the fire plume then an order of magnitude comparison (for a given geometric arrangement of inlets and extracts) is the first measure of the importance of one or other flow. That for the fire plume is,

$$\frac{Q}{\rho c \overline{\Delta T}_p}$$

and for the ventilation it is V/τ_r.

Substituting for $\overline{\Delta T}_p$ from equation (3.13) ventilation controls the flow in the enclosure when, to an order of magnitude,

$$K\ H^{5/3} \left[\frac{gQ}{\rho c T_\infty}\right]^{1/3} << \frac{V}{\tau_r} \qquad (3.16)$$

It is possible to define a fictitious heat release

$$Q_f = \frac{V^3\ \rho c T_\infty}{K^3 H^5 g \tau_r^3} \qquad (3.17)$$

The inequalities (3.15) and (3.16) become respectively

$$\frac{Q}{Q_f} >> \left[\frac{Q_n}{Q_f}\right]^{3/2} \qquad (3.18)$$

and

$$Q/Q_f >> 1 \qquad (3.19)$$

In addition to the above two inequalities the fire must exceed the effective background heating, ie

$$Q > \frac{Q_n}{N} \qquad (3.20)$$

where N is the number of separate heat sources assumed equal.

The above arguments are admittedly highly approximate and not without ambiguity but they illustrate plausibly considerations to be borne in mind and the basis for more detailed studies.

We can represent the results of the above discussion by Fig 3.3.

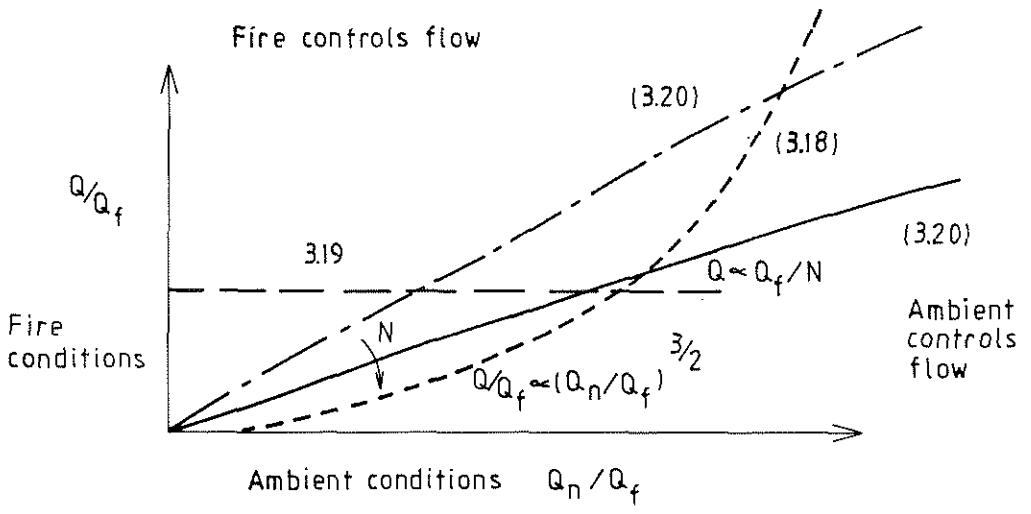

Fig 3.3 Diagrammic representation of dimensionless conditions for fire or ambient control of flow

3.3.2 Discussion of Criteria

The curved boundary in Fig 3.3 arises from criterion (3.18) in which Q_f appears on both sides.

In view of the above comments regarding approximation we cannot expect other than an order of magnitude estimate. Inequality (3.18) may be written as

$$Q >> K^{3/2} Q_n^{3/2} \left[\frac{g\tau_r^3 H^5}{V^3 \rho c T_\infty}\right]^{1/2}$$

and inequality (3.19) as

$$Q >> \frac{1}{K^3} \left[\frac{g\tau_r^3 H^5}{V^3 \rho c T_\infty}\right]^{-1}$$

The contrary roles of the group Q_f (when $Q \ll Q_n$) expresses the fact that high ventilation reduces the background heating but increases the background circulation.

In other words if there is background heating Q_n one could with low enough ventilation prevent a plume penetrating the hot layer that exists before the fire but a high enough ventilation would control the circulation. Suitably placed detectors might operate but the optimum position would depend on the ventilation and heating condition in the room as well as on the position of the fire.

There appears to be a limit for

$$\frac{gQ_n \tau_r^3 H^5}{\rho c T_\infty V^3}$$

above which a conventional two layer model cannot apply.

The analysis used here is relatively crude but appears plausible as a framework for more detailed studies or correlations of data. If we write $V = AH$ where A is room area and if we assume $Q_n \leq A$ or $Q_n \leq V$ but τ_r is constant with scale then $\frac{Q_n \tau_r^3 H^5}{V^3}$ varies between $\frac{H^3}{A^2}$ and $\frac{H^2}{A^2}$.

Spaces of large area would seem to be less dominated by ambient conditions but high spaces may be more affected.

The mean temperature rise in an enclosure can be translated into a pressure rise and compared with the external windeffect, measured as a velocity head. In terms of the above dimension variables Q/Q_f and Q_n/Q_f the effect of an external wind W_e is assessed by $W_e . \tau_r H^2/V$ with height again being an adverse and area a beneficial factor.

In order to derive some realistic value of Q_f let us assume

$\tau_r = 750$ s

$V = 150$ m^3

$H = 3$ m

and using the calculated value of $K = 0.22$ (based on $\alpha_o = 0.1$) Q_f becomes 0.11 kW. Calculating Q for smouldering fires, the data supplied by Quintiere can be used /19/

$Q = \dot{m} \Delta H$

where $\dot{m}$ is the rate of mass loss due to smouldering and ΔH is the heat of reaction. Experimental values for $\dot{m}$ and ΔH were quoted as

$$\dot{m} = ct$$

where $c = 0.206$ g/min^2 for polyurethane and $c = 0.33$ g/min^2 for cotton. Heats of reaction for the two materials are approximately 15 kJ/g and 11 kJ/g. (Other data in the same report give an order of magnitude lower values of ΔH). For polyurethane

$$Q = 3.1 \cdot t \text{ kW}$$

and for cotton

$$Q = 3.6 \cdot t \text{ kW}$$

with t in minutes.

This simple numerical example shows that for conventionally ventilated spaces the fire effect Q even for smouldering fires rapidly may overwhelm the ventilation effect Q_f. There is normally no significant effect of ventilation on the fire plume; background heating is much more important. The presence of ventilation rate to the cube power in Q_f expresses its well known importance for detection in "clean" rooms.

3.4 Experimental Modelling of Buoyant Flows

Burry /10/ has demonstrated physically many aspects of the effects of background heating by means of small scale flow studies. Local convectors can be moved about in a model of approximatly 600x600x1000 mm in which visible traces follow the flow and a classic demonstration shows the following pattern, see fig 3.4.

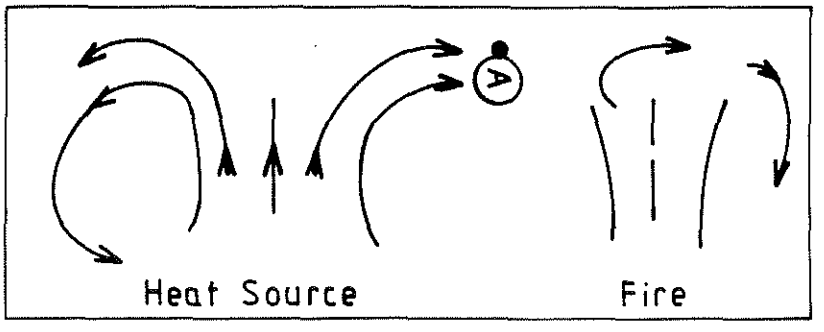

Fig 3.4 Operation of a detector may be delayed due to counter-current generated by non-fire heat source

He has also demonstrated that hot smoke flowing through the leak between door and combustible doorframe may cause a substantial pyrolysis of the frame material. As a consequence, the smoke in addition to being cooled becomes laden with

particulates. The density of the smoke aerosol may increase so that the leaking smoke actually is driven downwards towards the floor instead of forming a layer beneath the ceiling.

Such physical air based models or modelling using the mixing of liquids of different density can be used to assess various situations and various design of ventilation systems.

The reduced scale models be they liquid or air (with reduced heating) are particularly useful for visualising flows in complex geometries.

3.5 Numerical Modelling

Cox /11/, Morita /12/, Yamauchi /13/ and their co-workers are amongst those who have used numerical modelling to study smoke movement in enclosures. Yamauchi combined a field model with various smoke particle phenomena. Attempts are made to represent combustion in such models.

Computer aided modelling has the capacity to deal with the external boundary conditions of wind pressure, stochastically if so desired. It is for low temperature differences without combustion (other than that which can be represented by an energy source within well defined geometrical boundaries) that such modelling is so far best validated. Studies with the field model described in /11/ has started during winter 1987/88 in Lund.

4 SITING OF DETECTORS - SOME GENERAL CONSIDERATIONS

There are two aspects of siting, horizontal spacing and local separation from other objects near the ceiling. Johnson /14/ commenting on the Australian code points to the emphasis in the UK and US Codes on the need for close enough spacing in computer facilities with higher than normal ventilation.

The preferred horizontal spacing must vary with enclosure height. This will be discussed in more detail in chapter 7.

The drop in temperature and concentration due to dilution of a radially expanding ceiling jet must not be too large or the detector system will respond according to the position of the fire. The effective plume diameter at a height h above the heat source is about $2\alpha_0 h$, ie h/5, and this is the scale by which to judge horizontal separation.

Close spacing is intended to reduce the likelihood of the system being adversely affected by local ventilation currents, but costs rise.

Particular problems arise if there is a high level obstacle or high level heat source - eg electrical illumination.

Consider the formation of a layer and ceiling jet as in fig 4.1.

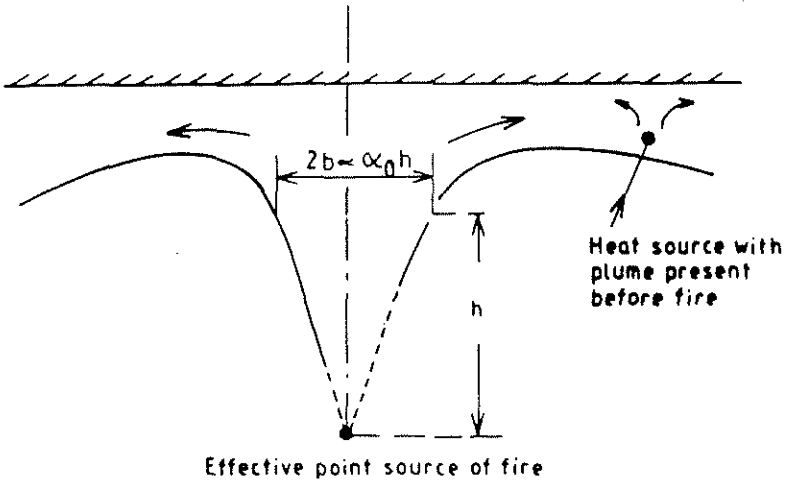

Fig 4.1 Pre-existing plume can assist mixing in hot gas layer

The initial depth of the layer will be roughly h/10 - the radius of the vertical plume - this layer gradually deepens as the hot gases are confined but clearly for conventional heights, around 2 1/2 m and upwards, the initial depth of layer will engulf most detectors. Consider an illuminated light bulb within the depth of this layer. The result of the ceiling jet already in existence from the bulb will be to inhibit the hot gases from the fire reaching the bulb but because the hot gas extends below the bulb parts of the layer will approach the bulb and be entrained into the bulb plume.

The bulb therefor simply mixes its local environment after perhaps an initial delay. A detector near the heat source might suffer some delay in operation until the layer has deepened so that no fresh air is entrained upward into the layer by the heated bulb, see fig 4.2.

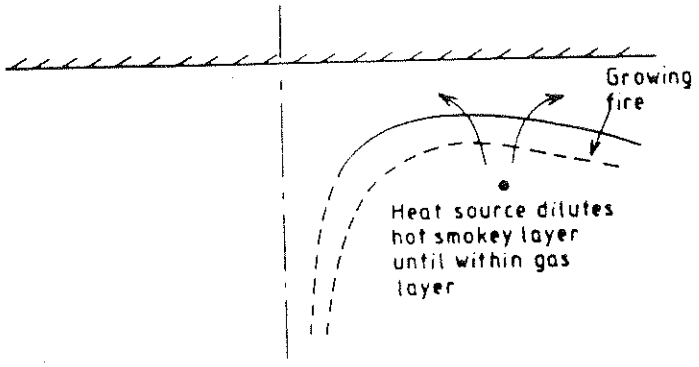

Fig 4.2 Heat source below hot gas layer dilutes layer and can delay operation of detection downstream

Vertical obstacles and recesses can produce recirculation zones which are not penetrated by the main stream. Detectors should therefore be sited clear of these.

Analogue or numerical modelling of local sites are tools for investigating such problems.

Johnson and Brown /14/ are amongst many who have studied the response of particular types of detector in domestic premises. They point out that the delay in detecting smoke in a bedroom from a fire that starts elsewhere could be too long to allow the occupants safe escape. A single smoke detector in a common hall is better and cheaper but, as Burry /10/ has observed smoke passing through door cracks into a common space may not necessarily go up.

5 FIRE DETECTOR RESPONSE

The presence of a fire will bring about various changes in the environment, which can be recognized by a fire detector (chapt.2 and 3). The four fire characteristics most commonly used for fire detection are Heat (convective), Flame Radiation, Gases and Smoke. Table 5.1 shows the common detector types used.

Table 5.1 Types of fire detectors

- HEAT
  - Point Detectors
    - fixed temperature
    - rate of temperature rise
  - Line Detectors
    - integrating
    - non integrating
- RADIATION
  - Ultra Violet Detectors
  - Infra Red Detectors
- GASES
  - Point Detectors
  - Line Detectors
  - Sampling Detectors
- SMOKE
  - Point Detectors
    - ionization chamber
    - light scatter
  - Line Detectors → light obstruction
  - Sampling Detectors
    - ionization chamber
    - light scatter

The performance of a fire detection system is very difficult to define quantitatively as the fire has many variable characteristics, most of which can not be fully predicted. Some detector types listed above are mainly used for special applications, where the performance criteria may depend on the particular application. The fire detection equipment must always be a compromise between its sensitivity to the fire, its propensity to give false alarms, its reliability and of course its cost.

The problem of evaluating the respons of fire detection devices can be split up into two physically separate categories. One is the response of the detector to a given source term immediately adjacent to the detector housing. The other concerns the transport of the fire signature to the detector housing. In this section the response of the detector to a given source term is discussed.The transport of a fire signature to the detector is discussed in Chapt 3 above.

5.1 Heat Detectors

In order to determine the time needed to raise the temperature of a heat detector from its initial temperature to its operating temperature, the thermal response must be known in such a way that it may be generalized for any given gas flow history. Heskestad and Smith /20/ developed an approximate model for heating of thermal sensing elements by fire driven flows. They found that for a wide range of sensors including commercial sprinklers, that the sensing elements may be considered uniform in temperature when heated by convective flow from a fire. Net radiative effects during early fire growth were calculated to be less than 20% of convective heating and may be neglected.With these approximations, the differential equation for sensing element temperature is /21/:

$$d(\Delta T_L)/dt = \tau^{-1}(\Delta T_g - \Delta T_L) \qquad (5.1)$$

where ΔT_L is the differens between ambient and detector temperature, and ΔT_g is the differens between ambient and fluid temperature. The time constant, τ, may be related to the properties of the sensing element and the convective heating of the gas flow according to:

$$\tau = m_L c_L / h_c A_L \qquad (5.2)$$

where m_L is the mass, c_L is the heat capacity per unit mass, A_L is the area of the sensing element, and h_c is the average convective heat transfer coefficient over area A_L.The time constant of the sensing element, τ, is not characteristic of the hardware alone because the value of h_c depends on the velocity of the gas flow. For detectors in crossflows, over the range of interest for detector operation, variations of the convective heat transfer coefficient are proportional to to the square root of gas velocity ($h_c \sim U^{1/2}$) and independent of the gas temperature .Therefor, the product of τ and the gas velocity to the half power is a characteristic of the hardware alone. Heskestad /22/ names this product the responce time index, RTI = $\tau_o U_o^{1/2}$,where the subscript, o, identifies reference test measurement conditions. The time constant at any gas velocity is calculated from the RTI using:

$$\tau = RTI/U^{1/2} \qquad (5.3)$$

Customary units for the RTI are $m^{1/2}s^{1/2}$. Values for the RTI range from 1 $m^{1/2}s^{1/2}$ for a thermocouple (diam=1mm) to 22 $m^{1/2}s^{1/2}$for quick operating residental sprinklers and 375 $m^{1/2}s^{1/2}$ for liquid filled bulb sprinklers /21/.

Point detectors operating at a fixed temperature are activated when the sensors reach a predetermined temperature. In its simplest shape the sensor consists of an alloy which melts at a predetermined temperature or of a bimetal-thermostat. The activation temperatures are usually 47, 57 and 70°C. A detector covers a floor area of about 40 m^2.

Point detectors operating at a fixed rate of temperature rise are activated when the temperature increases more than about 3 to 10°C per minute. The sensor usually consists of two thermocouples or semiconductors which are located in a way that one sensor is exposed to the air and the other is isolated. Fixed rate of temperaturerise detectors are activated at an earlier phase of a fire than fixed temperature detectors.

Line detectors can be constructed in different ways. Pneumatic tube type heat sensitive fire detectors are frequently applied for road tunnel protection. The practical advantages of this type of fire detecting system are a robust installation that is insensitive against electromagnetic interference and a fairly good fire detection capability.

Fig.5 1 shows a schematic sketch of a pneumatic tube fire detection system.

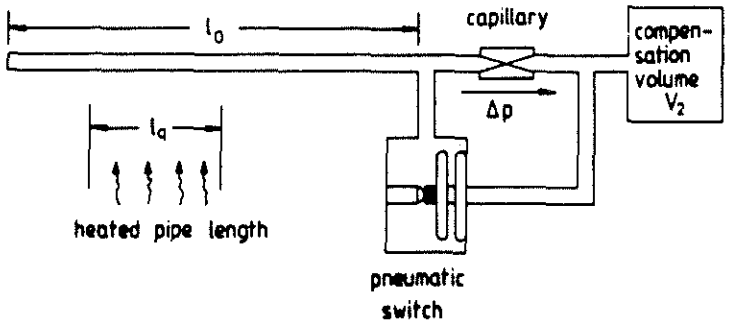

Fig.5.1 Pneumatic tube type fire detection system /23/

Ref /23/ presents a method to calculate the dynamic performance that is approximative as well but takes nonlinearities into account where it seems to be necessary. The method is limited to a time range of approximately 50 s and a response pressure treshold up to 400 Pa for the pneumatic switch.

5.2 Radiation Detectors

The established range of fire detectors such as ionisation chambers and light scattering detectors, although suitable for most applications, cannot provide adequate protection in certain situations. They are unsatisfactory in situations in which highly flammable material are stored indoors in large spaces or outdoors. In such situations a radiation detector can be used as it does not rely on convection or diffusion to convey the fire signal. Different aspects of these kinds of flame and spark detectors are given in ref /24-28/.

Radiation detectors operate by sensing the electromagnetic radiation from flames. Although a large part of the spectrum could be used, available detectors operate either in the ultraviolet region or one of three bands in the infrared region of the spectrum. In the visible region radiation due to natural light and various artificial lights interfere with the radiation from flames as shown in Fig 5.2 /24/.

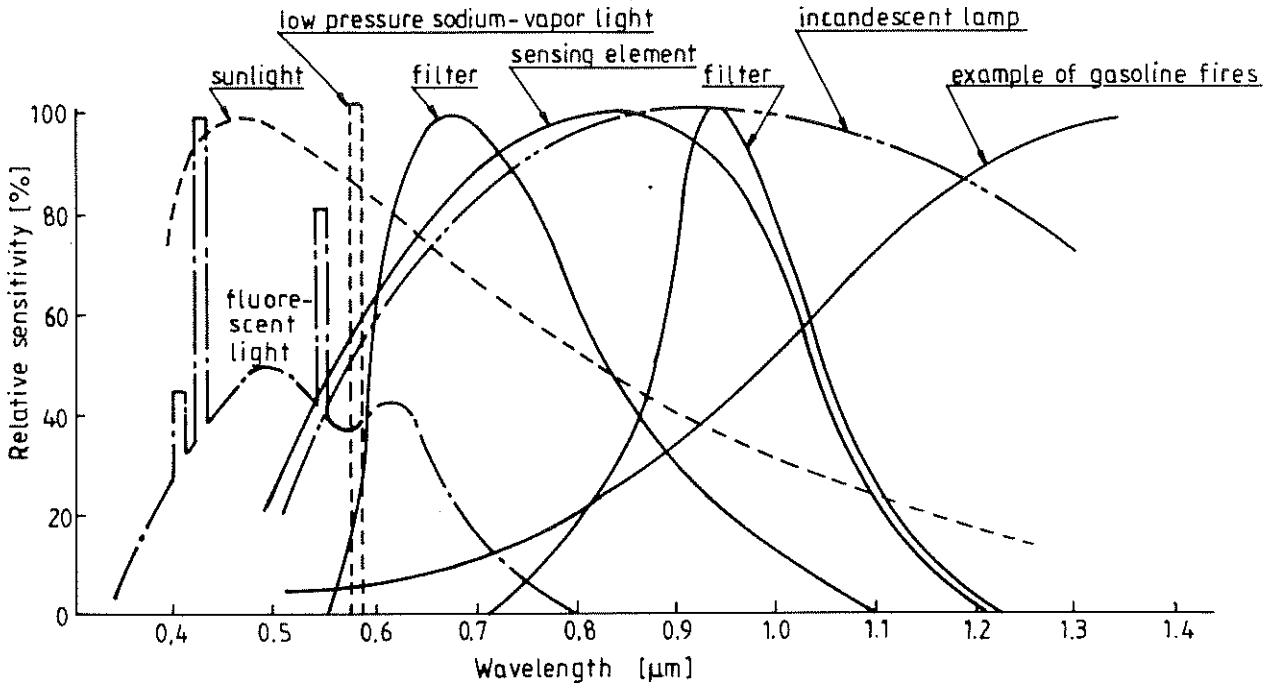

Fig 5.2 Spectral sensitivity characteristics /24/

5.2.1 Flame Radiation Characteristics

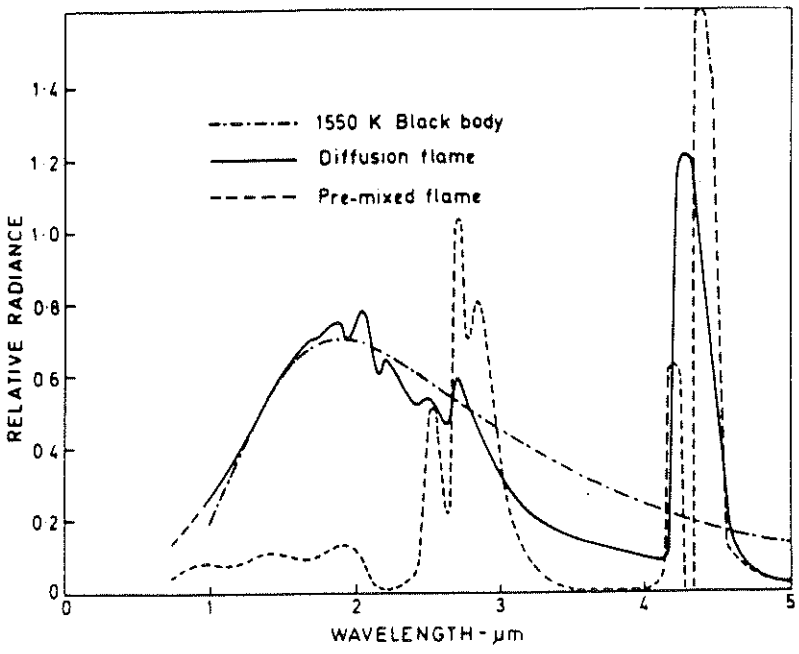

Fig 5.3 Flame spectra /25/

The different spectral content of diffusion flames and premixed flames are shown in Fig 5.3. The spectrum of a premixed hydrocarbon flame consists of a series of peaks corresponding to emission bands of the combustion products H_2O, CO and CO_2 (2μm; 2.7μm; 4.3μm; 6.7μm; 15μm:) and intermediates OH, CH, C_2,(280-300nm; 305-320nm; 385-395nm; 420-440nm; 460-570nm;). The diffusion flame shows emission and absorption bands as well but they are superimposed on the continuous spectrum of the radiation from the hot carbon particles. The radiation levels from an 0.1 m^2 petrol fire are approximately /26/:

$1 \cdot 10^{-7}$ $W.Sr^{-1}nm^{-1}$ in the ultraviolet region
$2 \cdot 10^{3}$ $W.Sr^{-1}nm^{-1}$ at the peak radiation around 2μm
$5 \cdot 10^{3}$ $W.Sr^{-1}nm^{-1}$ at the CO_2 emission peak at 4.3μm.

Another feature of the radiation from diffusion flames is that the level is not constant but varies about some mean level giving the well known flicker. The frequency of the flicker varies from 0.5 to 15 Hz. The modulation of the intensity level depends on the type of fuel and on what the detector is viewing. Typically the modulation will vary from about 20% for a small liquid fire to 5% for an open wood fire.

5.2.2 Ultraviolet Flame Detectors

The radiation from fires in the uv region is extremely small and detectors must therefore be higly sensitive. G-M tubes (Geiger-Muller) are commonly used as detectors. G-M tubes used are only sensitive to radiation having a wavelength shorter than 260 nm. The transmission of the glass envelope of the tube limits the response at shorter wavelengths giving a typical overall spectral response which lies between 185 nm and 245 nm. This feature makes the detector almost insensitive to solar radiation at ground level as shown in table 5.2 /27/.

The sensitivity of a uv detector varies with the distance as r^{-2}.The field of view is usually 90^{o} and a 0.1 m^2 petroleum fire can be detected at a range of 7-10 m.

However,the detection capability can be severely reduced by atmospheric attenuation and window contamination.Transmission of uv radiation through smoke is very poor and thus detectors should not look vertically down on potential fire risks. Various gases and vapours such as acetone,ethanol, toluene etc. exhibit significant uv absorption characteristics. Contamination of the G-M tube window by hydrocarbons such as oil or grease can significally reduce the detector's performance.

The major cause of false operation with uv detectors is welding. Welding produces a very high intensity signal and detector operation can occur at distances of two or three kilometers from the welding sourse.

Table 5.2 /27/

Summary of background radiation and radiation from test lamps

Wave lengths (nm)						
Source	180-250	250-300	300-350	350-400	400-450	Note
Direct sun	1	18	55	90	145	3)
Daylight		0.5	4	60		3)
Glow lamp		0.01	0.4	3.2	11	1)
Fluorescent tube		0.03	0.5	1.4	4.2-13.0	2)
Deuterium lamp	$7.5 \cdot 10^3$-$18.5 \cdot 10^3$-$7 \cdot 10^3$-$5 \cdot 10^3$-$1.3 \cdot 10^3$-$1 \cdot 10^3$					1)
Xenon high pressure lamp	$1.1 \cdot 10^3$-7.10^3-$1.4 \cdot 10^4$-$1.9 \cdot 10^4$-$2.5 \cdot 10^4$-$3.25 \cdot 10^4$					1)
OX4W	$0.2 \cdot 10^3$-$0.2 \cdot 10^3$-$20 \cdot 10^3$-$0.9 \cdot 10^3$-$0.9 \cdot 10^3$-$2.2 \cdot 10^3$					2)
Standard UV	$0.5 \cdot 10^3$-$2 \cdot 10^4$-$3.6 \cdot 10^4$-$7.8 \cdot 10^4$-$1.2 \cdot 10^5$-$1.3 \cdot 10^5$					

1) Values in $\mu W/cm^2/nm/sr$

2) Values in $\mu W/cm^2/sr$ (most intensive lives for standard UV)

3) Values in $\mu W/cm^2/nm$

5.2.3 Infrared Flame Detectors

Infrared detectors operating in different spectral bands have appeared in several forms dependent on operating requirements and the availability of suitible detectors, Fig 5.4 /25/.

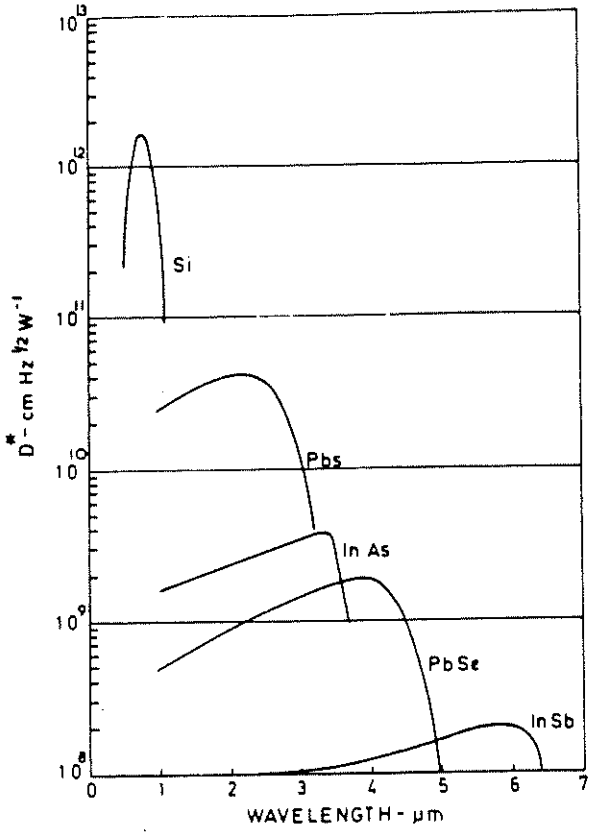

Fig 5.4 Spectral detector sensitivity /25/

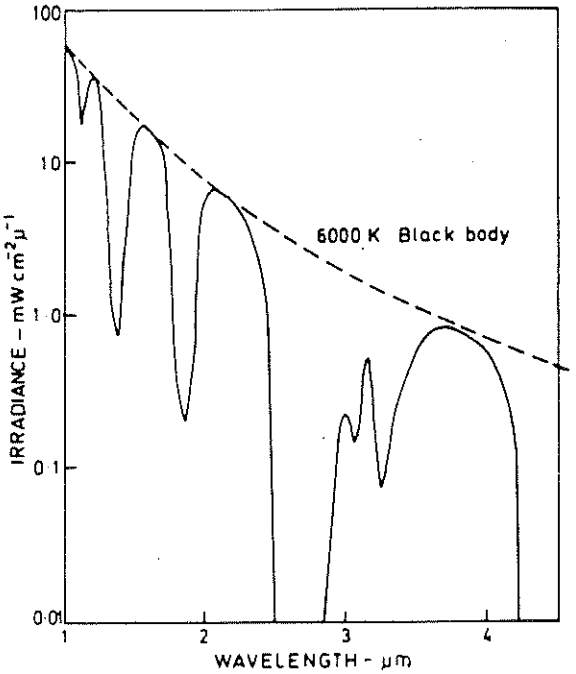

Fig 5.5 Solar spectrum, ground level, 45° zenith /25/

It is clear from fig. 5.4 that the detectivity achievable falls rapidly with increasing wavelength.

The solar radiation contributes usually more to the background radiation than the man made sources. In regions away from the strong absorption bands in the solar spectrum, as shown in Fig.5.5, the irradiance due to direct sun-light is approximately two orders of magnitude greater than the irradiance of a fire of 0.5 dm^2 at a range of 30 m, which is considered to be typical of the fire which a system must be designed to detect. Indirect solar radiation can also be a problem since it will generally orginate within the area to be protected.

The irradiation reaching the detector will be subjected to attenuation. The main sources of attenuation are atmospheric, by aerosols and windows. The atmospheric attenuation, shown in Fig.5.6 is caused by strong absorption bands in water vapour and carbon dioxide, i.e. the same bands at which the combustion products radiates. Due to the temperature difference between the combustion gases and the surrounding atmosphere the energy levels are populated differently which means that there are not a complete overlap between the emission spectra from the combustion products and the atmospheric absorption.

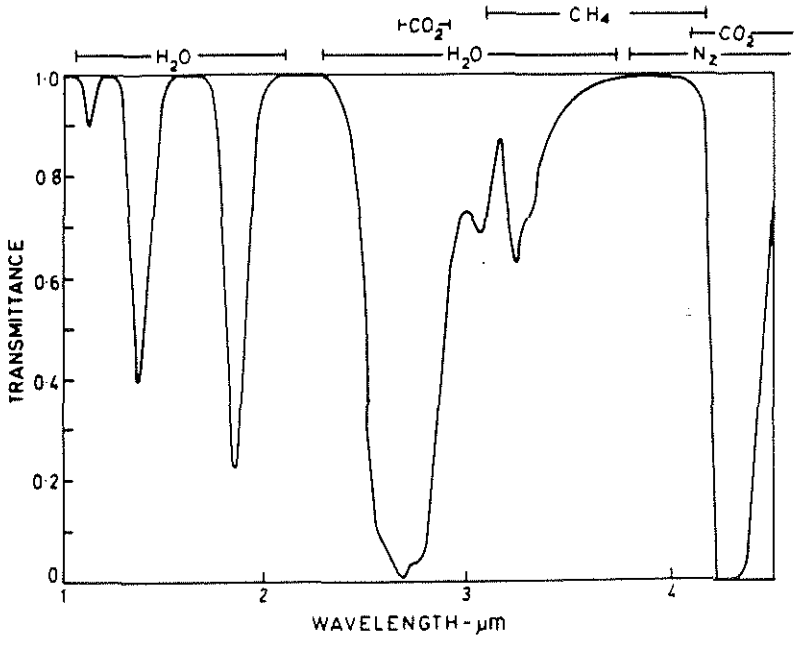

Fig 5.6 Atmospheric absorption, 100 m path /25/

Early detectors operated in the 1μm region using silicon cells and were designed for use in indoor environments only. Detectors are also available working in the 2.7μm CO_2 absorption band, using lead sulphide as the sensing element. They are not completely blind to solar radiation. More recently a number of detectors have appeared operating in or around the

4.3μm CO_2 absorption band. Most of these detectors use a two sensor system, each sensor looking at a different part of the infrared spectrum, in order to achieve discrimination against solar and background radiation. However one detector uses a single sensor and achieves complete blindness to solar radiation by optical means only. These detectors approach the ideal flamedetector specification.

5.3 Gas Sensors

Combustion gases from fires contain a lot of components that do not occur in ordinary air. Some gases produced are specific for the fuel and other such as hydrocarbons, hydrogen, carbon monoxide and dioxide, are common to most fuels and thus suitable for detection. The presence of carbon dioxide in ordinary air makes the signal to noise ratio too low to be used as a detector signal. Thus the obvious choice would be detection of hydrocarbons, hydrogen and carbon monoxide for a gas detection system. The sensivity ought to be in the 10-100 ppm level.

A new approach is proposed as an alternative /29/, in which additives that act as a latent sensory warning agents of slow, smoldering combustion or overheating are incorporated into textiles, foams and plastics. However a commercial system is not available.

A lot of different analytical instruments are available that are capable of detecting combustion gases such as unburned hydrocarbones and carbon monoxide in the 10 to 100 ppm level, for example flame ionisation detectors, mass-spectrometers, I-R absorption with gas correlation. However, these instruments are not suited as gas detectors for fire alarms. They are too expensive and not suited to operate continuously for three to five years without zero correction.

A development of new solid state detectors for fire alarms is under way /30/. The electrical resistans of certain metal oxides such as tin oxide are at elevated temperatures strongly dependent on the presence of oxidable gases and the gain in certain silicon semi-conducters is strongly dependent on the presence of hydrogen in the atmosphere.

The rapid development during the last years of diod lasers, optical fibers, electronics and microcomputers will facilitate the development of new optical absorption gas sensors.

5.4 Smoke Detectors

5.4.1 Ionization Chambers

The use of ionisation chambers as smoke sensors is well known and the associated theory outlined in the litterature /31-32/. The working principle for the ionization chamber for smoke density measurements is shown in Fig 5.7.

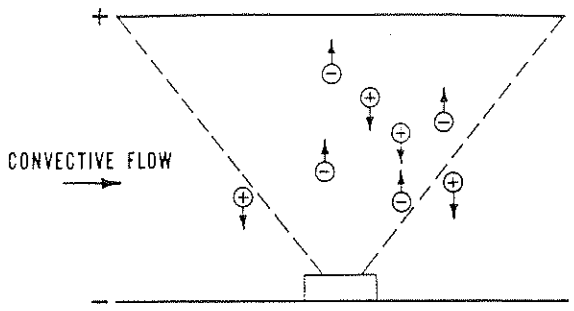

Fig 5.7a) Working principle for ionisation chamber, without smoke

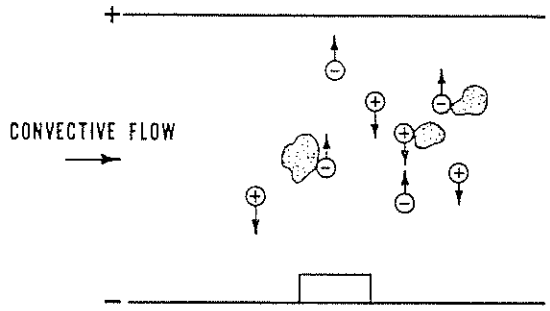

Fig 5.7b) Working principle for ionisation chamber, with smoke

The chamber consists of a source of ionizing radiation positioned between two electrodes across which an electric potential is maintained. The radiation source emits alpha particles or beta particles at relatively high energies, creating positive ions by removing electrones from gas molecules along their path. The low energy electron released rapidly attaches to a neutral gas molecule which becomes a negative ion. These ions are then drawn to the electrodes where they give up their charge. This charge transfer represents a small ($\approx 10^{-11}$ A) current flow, I_o, through the air space between the electrodes, Fig 5.7a. When smoke particles enter the chamber, these particles capture ions, reducing their velocity by several orders of magnitude due to the increased mass of the particle-ion pair. This reduced velocity allows the pair to be carried from the chamber before reaching the electrode, reducing the charge transfer and thereby the chamber current, Fig 5.7b. It is this reduction in current, I, which is used to trigger the alarm.

Hosemann /33/ derived a semi-empirical equation for the relative chamber signal of a bipolar ionization chamber and Scheidweiler /34/ gives this equation as:

$$(I) \qquad X = (I_o - I)/I_o = N \cdot D_p/(2\eta) + 1 - \sqrt{((N \cdot D_p/(2\eta))^2 + 1)} \qquad (5.4)$$

where $\eta = (3 \cdot \sqrt{(\alpha_c \cdot q)})/C$ = chamber constant

X = relative chamber signal = $(I_o - I)/I_o$

N = number of particles of size D_p

D_p = particle diameter

α_c = recombination coefficient

q = ion generation rate

C = Bricard capture coefficient

For low concentrations of a smoke aerosol equation (I) reduces to :

(II) $X \sim N \cdot D_p$ for a monodispersive aerosol and (5.5a)

(III) $X \sim \Sigma_i (N_i \cdot D_{p_i})$ for a polydispersive aerosol (5.5b)

Thus the respons, X, is proportional to the diameter of the particle D_p as shown in Fig 5.8 /31/.

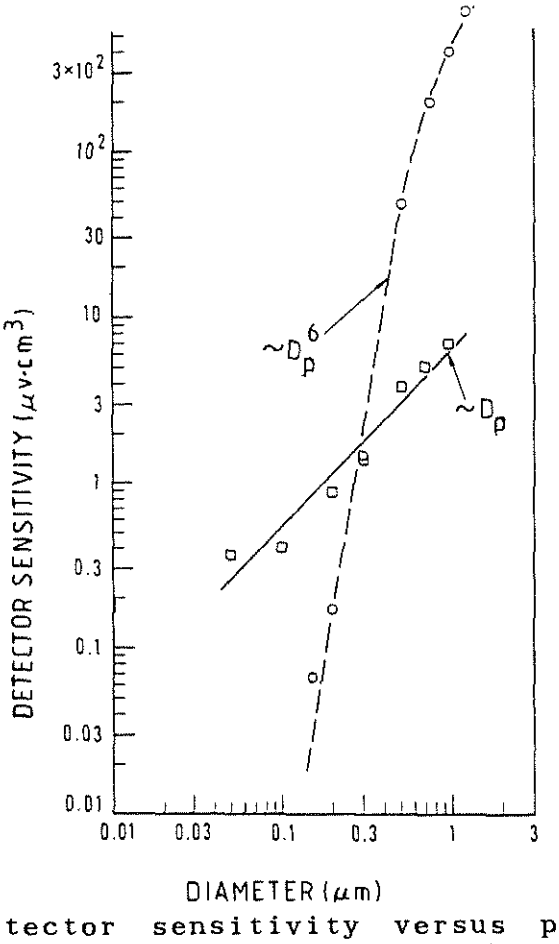

Fig 5.8 Detector sensitivity versus particle size for a light-scattering type detector, S-2, and for an ionization type detector, R-2 /31/

When using this general relation, one must keep in mind that an aerosol particle size distribution is dynamic, varying with time and distance from the generation source. The particle diameter will tend to increase due to coagulation effects which are related to time and concentration. Also, particularly in combustion aerosols, the particle size distribution being generated can change as a function of temperature of combustion, material and its density, moisture content, and other factors. In Fig 5.9 the particle size distribution for smoke from α-cellulose is shown under flaming and non-flaming exposure conditions /2/.

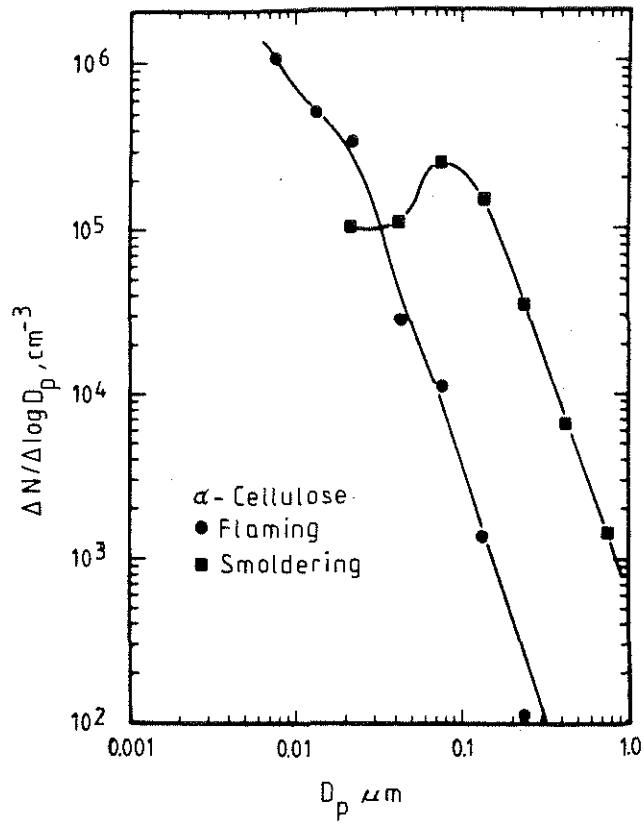

Fig 5.9 Smoke from α-cellulose under flaming and non-flaming exposure conditions /2/

If one assumes that the coagulation is spherical it can be seen that the number concentration N_d for a fix mass concentration is inversely proportional to the diameter cubed, D_p^3. As the relative chamber signal according to III is proportional to $N_d \cdot D_p$ the overall effect would be a reduction of the relative chamber signal by a factor of D_p^{-2}. Thus ionisation chambers become less sensitive as the smoke is aged as shown in Fig 5.10 /31/.

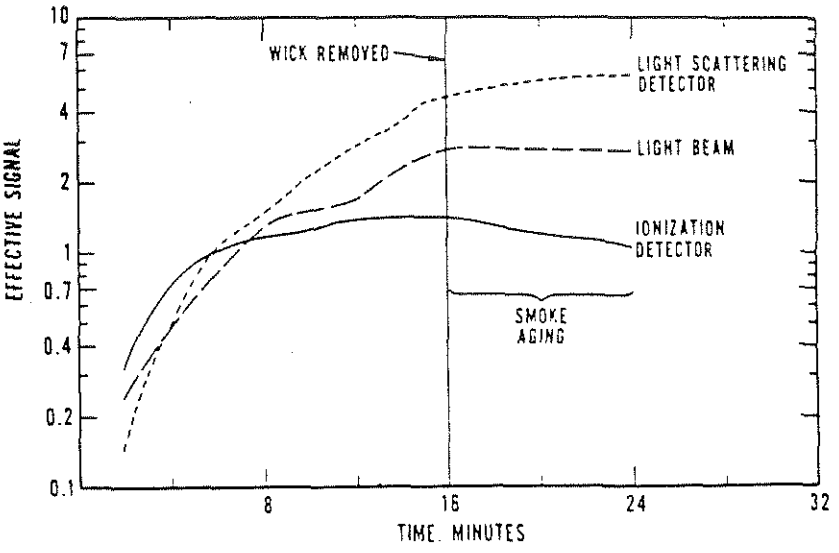

Fig 5.10 The effect of aging on smoke detector response /31/

Since the basic principle of operation of the ionization chamber detector involves a small flow of current created by transfer of charge across the chamber, any factor which interferes with this change will affect the chamber current and therefore the response. Some factors which interfere are air velocity, relative humidity, air temperature, air pressure, source strength, distance between chamber electrodes, and vapours and gases. Thus there is a need for a standard measuring instrument which is applicable for smoke density reference measurements. The reference chamber proposed as a common European standard is the so called MIC /35/ (MIC 527 and MIC 528). The relative chamber signal, X measured by the MIC 528 reference chamber for example is called the MIC-value.

5.4.2 Photoelectric Detectors

Optical techniques can be applicable for particle sizing. The methods used for smoke detection are based on light scattering and extinction. Most detectors in common use operate on the light-scattering principle as shown in Fig 5.11.

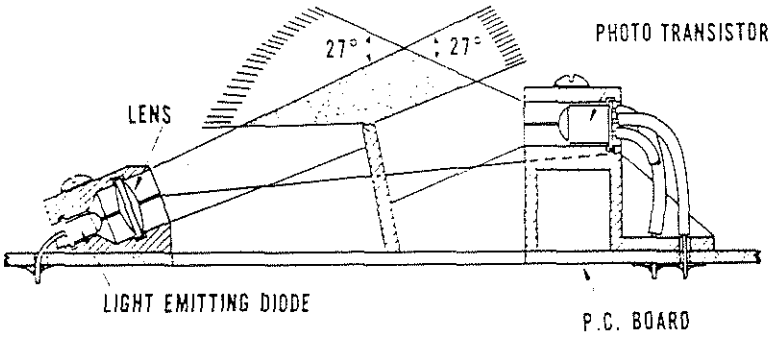

Fig 5.11 Light-scattering detector optics /31/

Light-scattering and absorption due to particles can be treated as a complicated boundary value problem in the electromagnetic theory.

Assume a plane polarized wave , wavelength = λ, incident on a homogeneous sphere, with diameter d, dielectric or conducting, Fig 5.12.

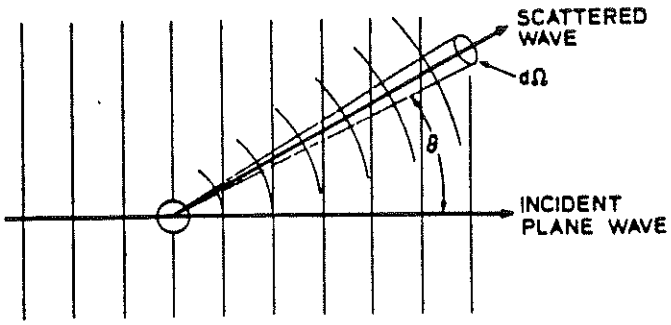

Fig 5.12 Plane polarized wave incident on a homogenous sphere

The solution is a function of:

size parameter $\alpha_s = \pi \cdot d/\lambda$

scattering angle θ (measured from forward direction)

complex refractive index $\bar{m} = (m+im')$ relative to medium

polarisation: E-vector $\parallel$ or $\perp$ to plane of observation φ

Define angular scattering efficiency per particle as

$$\frac{I_{\parallel}(\theta,\alpha_s,\bar{m})}{I_{\perp}(\theta,\alpha_s,\bar{m})} = \frac{\text{power scattered per steradian at angle } \theta}{\text{power incident on particle (projected area)}}$$

and extinction efficiency per particle (integrated over 4 π)

$$E(\alpha_s,\bar{m}) = \frac{\text{power scattered and absorbed by particle}}{\text{power incident on particle (projected area)}}$$

Theory gives these quantities as infinite sums involving Bessel functions and Legendre polynomials. The results can be divided into three regims, small, intermediate and large particles.

		for $\lambda \approx 0.5\mu m$
Small : Rayleigh limit	$\alpha_s \leq 0.3$	$d \leq 0.05\ \mu m$

simple analytic results

Intermediate: Full Mie calculations necessary $\quad 0.3 \leq \alpha_s \leq \frac{3}{\bar{m}-1} \quad 0.05 < d \leq 2\mu m$

Large: Approximation as diffraction+reflection+refraction $\quad \alpha_s \geq \frac{3}{\bar{m}-1} \quad d > 2\mu m$

In Fig 5.13 - 15 scattering and extinction efficiency for spherical particles are shown for the three regimes.

A RAYLEIGH SCATTERING ($\alpha_s < 0.3$)

$$I_\perp(\theta) = \frac{\alpha_s^4}{4\pi}\left|\frac{\bar{m}^2-1}{\bar{m}^2+2}\right|^2 \quad ; \quad I_\parallel(\theta) = I_\perp \cos^2\theta$$

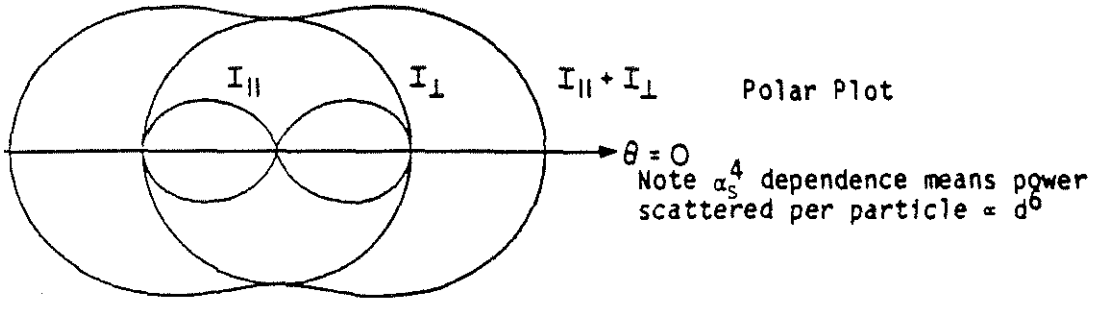

Fig 5.13 Rayleigh scattering, small particles

$$E = 2\pi \int_0^\pi (I_\parallel + I_\perp)\sin\theta d\theta = \frac{8}{3}\alpha_s^4\left[\frac{m^2-1}{m^2+2}\right]^2 \quad - \text{ m real}$$

For absorbing spheres $E \approx 4\alpha_s \, \mathrm{Im}\left[\frac{\bar{m}^2-1}{\bar{m}^2+2}\right]$

Thus absorption dominates in the Rayleigh Limit if $\bar{m}$ not real.

B INTERMEDIATE SIZE - MIE THEORY

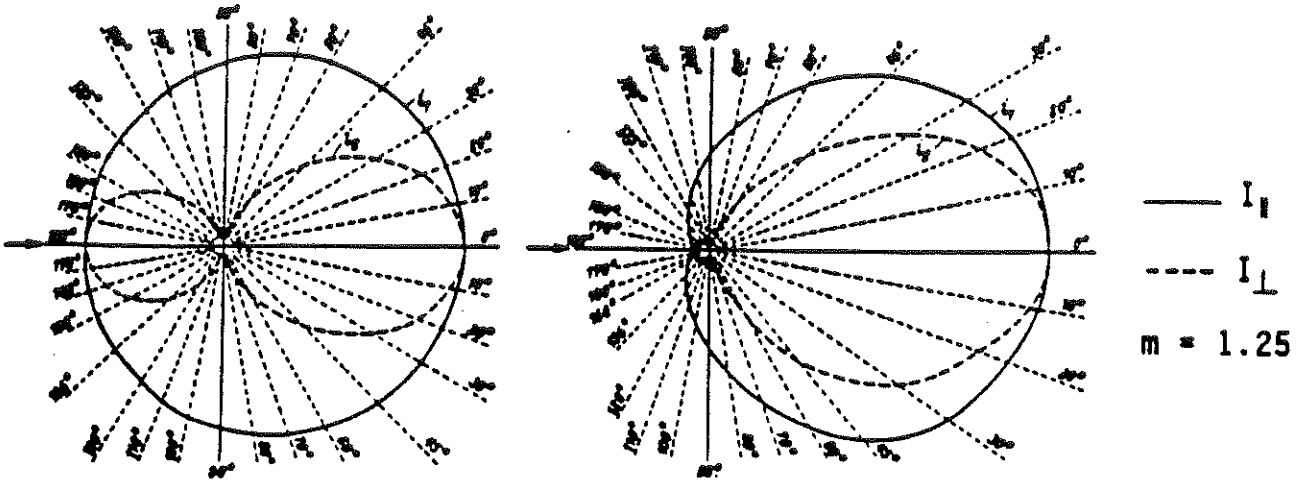

Fig 5.14 Mie scattering, intermediate particles

Fig 5.14 shows that as α_s increases above 0.3, the scattering efficiency increases less rapidly than α_s and the pattern becomes increasingly forward directed.

Extinction efficiency E (α_s, $\bar{m}$) from Mie theory is described by Fig 5.15.

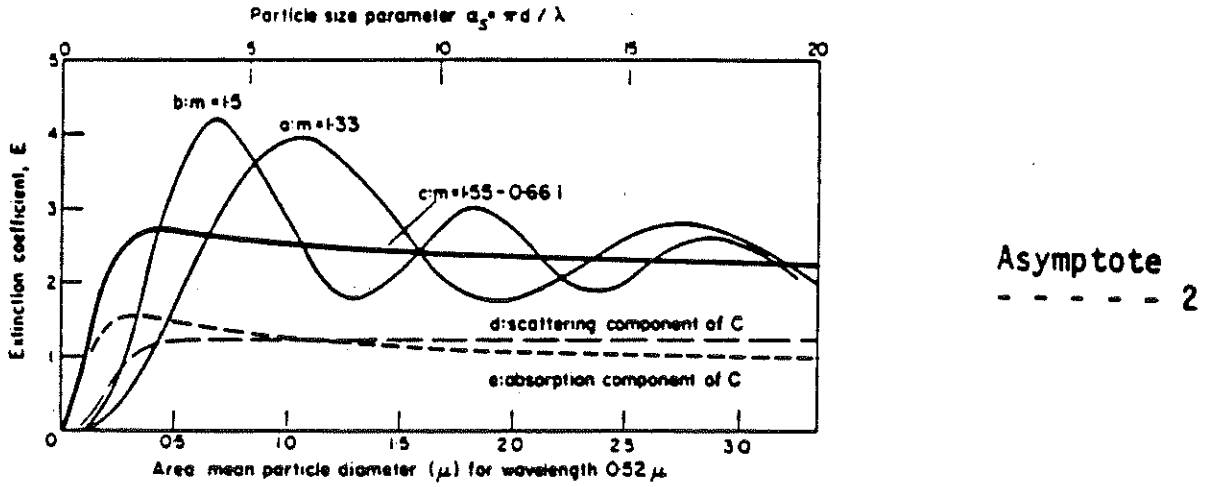

Fig 5.15 Extinction efficiency from Mie theory, intermediate particles

If the refractive index $\bar{m}$ is real (m' = 0), E (α_s) increases as α_s^4 for small α_s, then more slowly reaching max $\approx$ 4 at $\alpha_s \approx$ 2/(m-1) then shows damped oscillations to asymptote E = 2.

Absorbing particles (soot) show $E \sim \alpha_s$ for small α_s; the oscillations are damped. Roughly half the extinction is due to scattering, half to absorption.

C LARGE PARTICLES

Extinction efficiency is described by the equation

$$E(\alpha_s, \bar{m}) = 2\pi \int_0^{\pi} (I_{diff} + I_{refl} + I_{refr}) \sin\theta d\theta = 2$$

Thus, according to approximate theory, half the extinction is due to diffraction in the narrow forward lobe. The other half is due to reflection and refraction (or absorption) and is spread out over 4π representing the side and back-scattered lobes of the full Mie theory. For a size or wavelength distribution over a range $\geq$ 2:1, the approximate theory is adequate and much simpler than integrating the Mie results over the distribution.

From the figures above the sensitivity of light scattering and extinction detectors can be derived.

5.4.2.1 Light Scattering

The scattered light from small particles is very low but increases with D_p^6 as shown in fig 5.8. As α_s grows above 0.3 ($D_p \approx 0.05$ µm) the scattering efficiency increases less rapidly and the pattern becomes increasingly forward directed. If one assumes that the coagulation is spherical it can be seen that the number concentration N_d for a fix mass concentration is inversely proportional to the diameter cubed, D_p^3. As the scattering intensity increases as $N_d \cdot D_p^6$ the overall effect would be an increase in signal by a factor of D_p^3. Thus light scattering becomes more sensitive as the smoke is aged as shown in fig 5.10 above.

5.4.2.2 Light Extinction

The extinction coefficient is proportional to D_p^3 for small particles ($D_p < 0.5$ µm) and to D_p^2 for larger particles ($D_p \geq 0.5$ µm). If one assumes spherical coagulation as above the extinction signal for a fix mass concentration will be independant of the particle size distribution for small particles and proportional to D_p^{-1} for larger particles. Thus light

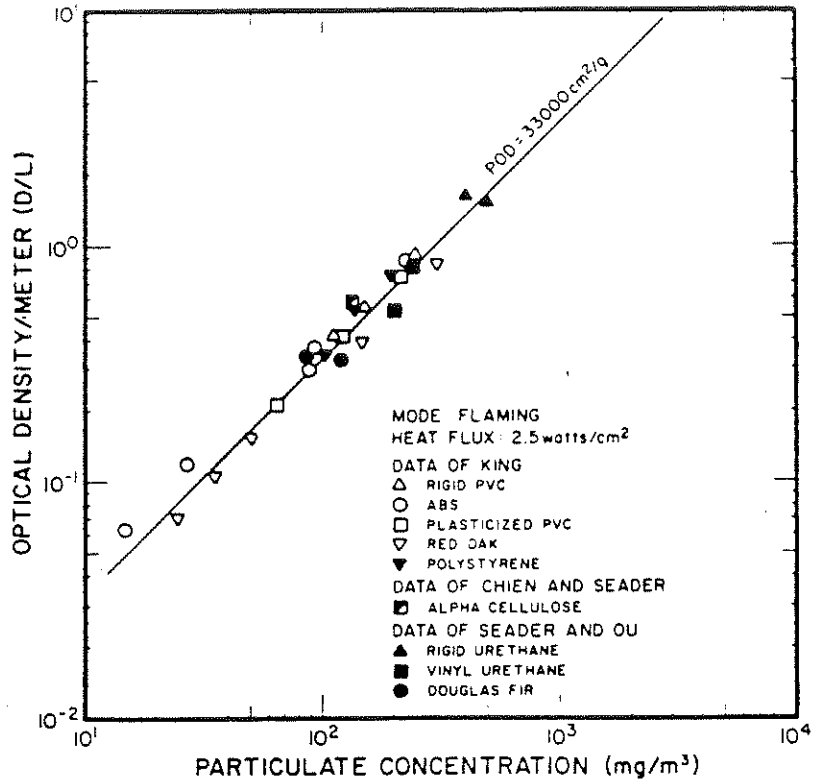

Fig 5.16 Correlation of experimental data on particulate optical density for flaming mode /4/

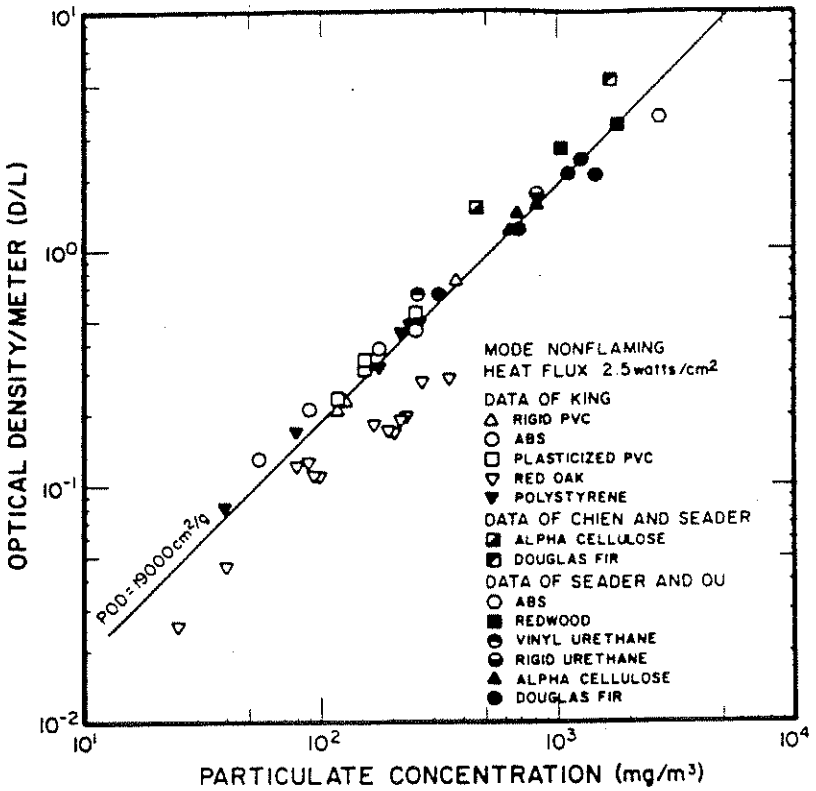

Fig 5.17 Correlation of experimental data on particulate optical density for nonflaming mode /4/

extinction is approximately independent of smoke aging as shown in Fig 5.10 above. This means that there is a correlation between particulate concentration and the extinction measured as optical density per meter. The correlation, however, is dependent on the refractive index of the particles. Flaming and nonflaming modes give different correlations as shown in Fig 5.16 - 5.17.

The theory above concerns spherical particles. The effects of complex aerosol shapes are largely unknown. One can empirically determine the effective scattering cross section of a complex shaped particle but this parameter can change continuously as the particle tumbles randomly in an aerosol stream. If the aerosol concentration is high enough, it is valid in many cases to assume a random distribution of particle orientations.

5.4.3 Test Standards for Smoke Detectors

The proposal for a Swedish test standard for smoke detectors /SMS, remiss 1415,1986/ follows the European standard. The standard covers smoke detectors that operate using scattered light, transmitted light, or ionization. In the fire sensitivity classification the detector is exposed to six different fires, open cellulosic fire (wood), smouldering pyrolysis fire (wood), glowing smoldering fire (cotton), open plastics fire (polyurethane), liquid fire (n-heptane) and liquid fire (met-hylated spirits).

6 FALSE ALARMS

Possibly the most pressing problem regarding fire detection concerns the false alarm situation. A very recent note in "Brand och Räddning" /36/ highlights the situation: During 1986 in Gothenburg 92% of the 1 597 alarms relayed to the fire brigade were false.

Section 6.1 will review some of the statistics regarding false alarms and 6.2 some of the remedies that have been applied and their quantitative effects.

6.1 Statistics

False alarms are widely acknowledged as a major problem in alerting people to danger.

Watanabe, Sasaki and Unioki /38/ state that in the 1960's the gross rates of false alarms to real alarms was 3.9:1 in Japan and give two values both over 10:1 in the 1970's for England /39-40/. In Sweden Malmö fire brigade has followed the statistics of false alarms during the 1966-1986 as shown in Fig 6.1.

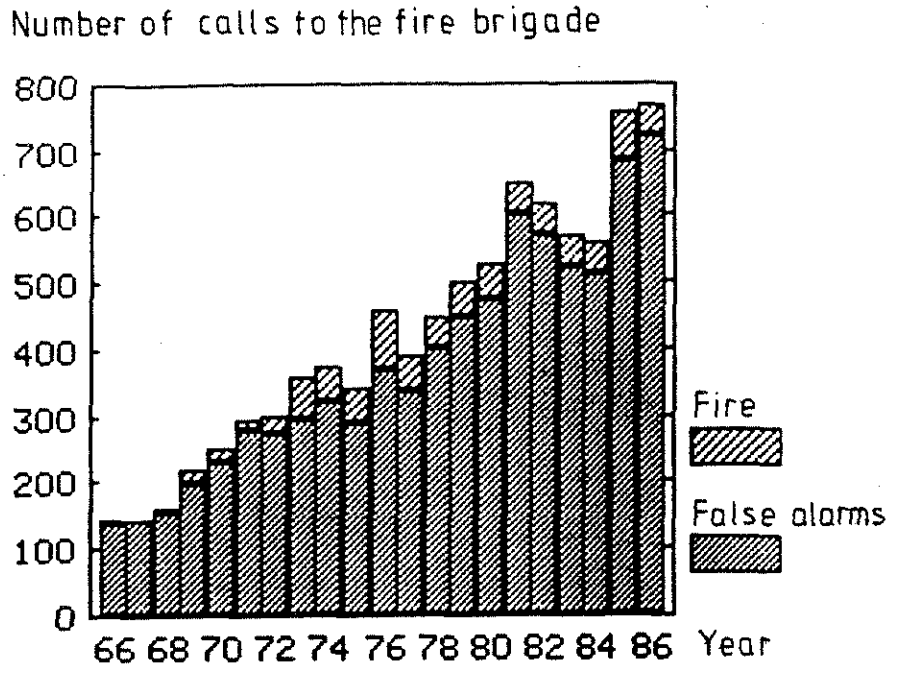

Fig 6.1 Alarm statistics in Malmö 1966-1986. (Ca 20.000 detectors, mainly smoke, in 1986)

As shown the gross rate of false to real alarms has been in the bracket 10:1 - 15:1 during the whole period.

Watanabe et al state that the probability of false alarm per detector and year in Japan is 0.065 for smoke and 0.008 for heat detectors. Fry /40/ is quoted by Breen /41/ as giving

0.05 in the early 1970's for all UK detectors and Breen himself gives, in 1985, 0.25 in a particular occupancy in the USA. This high value was attributed by Breen to greater sensitivity of the detector head and was in fact reduced significantly by desensitizing the smoke detectors. In Malmö the probability of false alarm per detector was approximately 0.04.

Clearly, higher sensitivity and the coupling of several detector heads to one system aggravated the false alarm problem. On the other hand lower sensitivity results in delayed or no alarm. Watanabe el al state that in buildings in Japan where automatic fire systems are installed, 76% of total fires during 1976 to 1981 were successfully detected by automatic fire detection systems. In the remainder, 15.4% of total fires occurred where no fire detector was installed, and 8.7% could not be detected by the automatic fire detection systems.

The reason for false alarms varies. Watanabe et al describe a statistical analysis and refer explicitely to the roles of smoking and cooking, factors which might well be expected to a different degree to apply outside Japan. However, 1/3 or more of the false alarms could not be attributed to a particular cause. Burry et al /42/ have studied the temperature variations in a room over a long period and could predict the rate of false alarms for thermal detectors as function of temperature increase per time, deg $^{o}C.min^{-1}$, as shown in Fig 6.2.

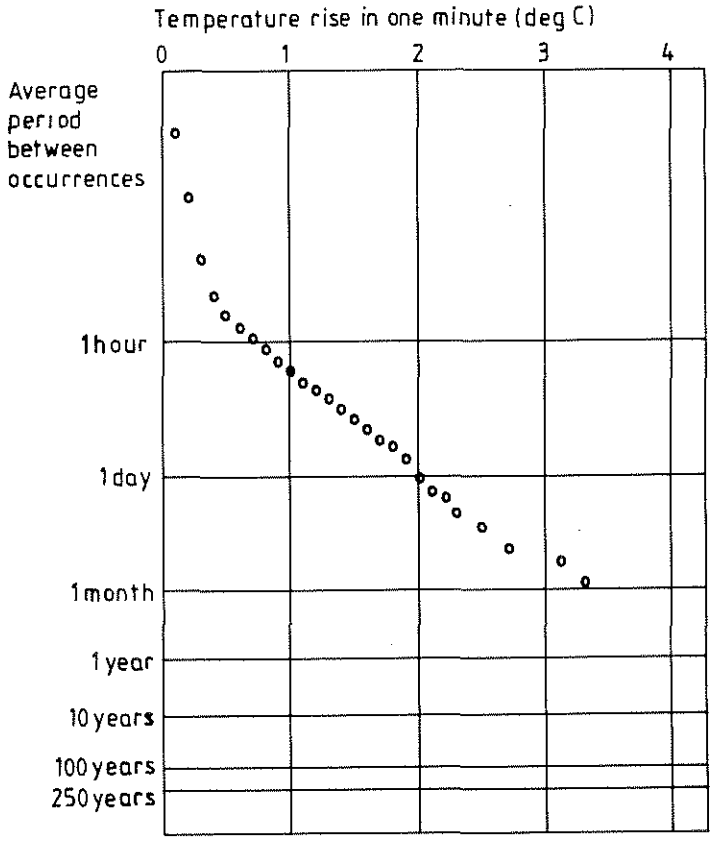

Fig 6.2 Ambient study: rate of rise of temperatur /42/

In Malmö a statistical analysis of false alarms has shown, Fig 6.3, that technical malfunctions, transfer/tele and smoke from welding, cutting, vehicles and tobacco are the main reasons for false alarms.

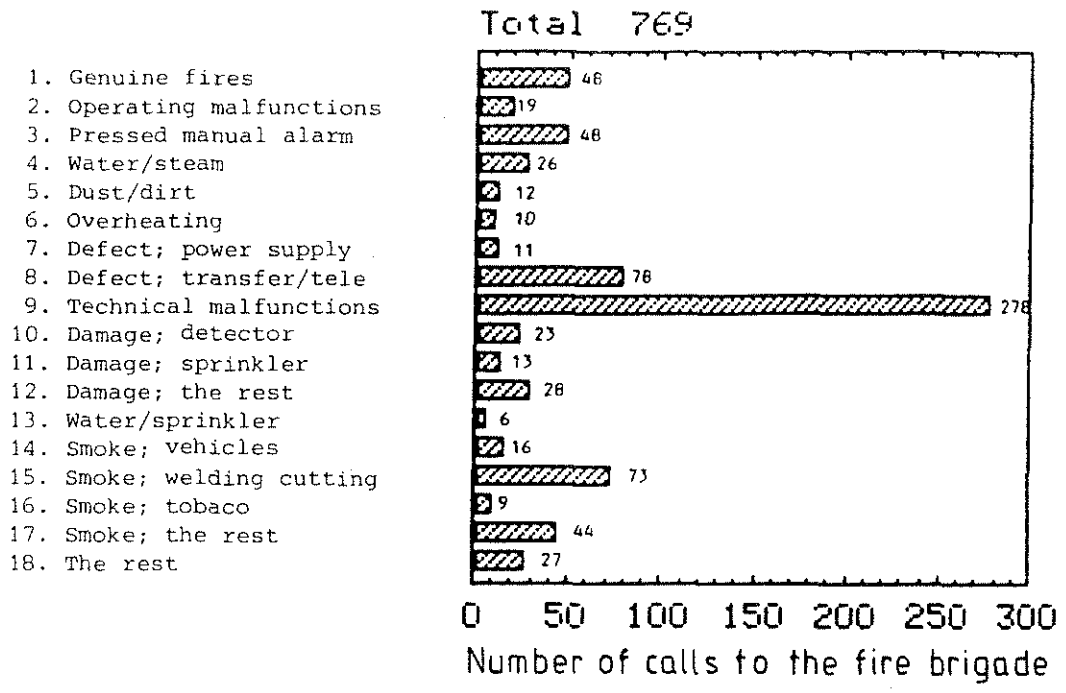

Fig 6.3 Reasons for false alarms in Malmö 1986 (Ca 20.000 dectectors)

It is not clear what vould be an acceptable false alarm rate except that it presumably differs according to circumstances. An individual in a lifetime is unlikely to experience a fire whilst in a small building. A few false alarms will probably not significantly alter his or her surprise at any alarm false or real. In a hotel or other large occupancy building the probability of any alarm is higher and the management or fire brigade to which the alarm system is connected will react against a sequence of false alarms.

The technical development in automatic fire detection is mainly governed by the rapidly increasing development of electronic components including microprocessors that opens a variety of new signal processing tools /43-45/. Most applications used in automatic fire detection systems are aimed at the improvment for system handling in the alarm or in the fault signal situation or at the improvement of automatic system monitoring. In large systems addressability can make a system cheaper by reducing cabling costs. The ultimate in this direction is a wireless alarm system in which radio transmissions are substituted for conventional hard wiring. Johnston /46/ remarks that the problems of spurious alarms from external radio sources needs to be overcome.

The most sophisticated of recently installed systems in Japan, able to address an individual detector gave a false alarm probability of 0.0015 per year per detector.

The Australian system described in /14/ is claimed to achieve its balance between false alarms and at a higher level of sensitivity than do conventional smoke detectors. Partly by having more than one level of operation and partly by employing a sampling and integrating principle which exploits the high sensitivity of the equipment.

No data have been found separating faults arising from the sensing elements false response and those from the circuitry. Johnson /46/ quotes Bukowski that the compromise between sensitivity and false alarms is not the same in the USA, Japan and the UK.

6.2 False Alarms and Possible Remedies

A large amount of information is available regarding false alarms and remedial actions. Most of it is qualitative, but recently reports have been published describing in quantative terms the effectivness of various measures. Some of the relevant reports are summarized below.

6.2.1 The ELAB Report /47/

The report recapitulates the information from 12 investigations on false alarms causes and frequencies. From these and other sources the report lists a range of possible counter-actions, divided into three sectors: measures related to detector environment - type and location, active measures and measures related to building category.

6.2.1.1 Measures Related to Detector Environment - Type and Location

An extensive table (30 types of environmental factors and detector location are matched against 10 types of detectors) indicates the combinations likely to cause an excessive number of false alarms. It is pointed out that a rational use of this information when designing and installing new systems could result in substantial false alarm reductions.

6.2.1.2 Active Measures

The report lists a number of strategies.

1. Testing period. Every installed system should be improved and tuned during an introductory trial period (duration perhaps 1 year) during which the automatic larm transmission is discontinued.

2. No alarm is transmitted until at least two detectors have activated.

3. Automatic compensations for regular variation in ambient temperature or changed sensitivity due to dust deposition, etc.

4. Alarm verifications procedures. No alarm is transmitted until a number of signals received have indicated a continuous state of alarm.

5. Self checking procedures with respect to integrity of electric circuit, etc.

6.2.1.3 Measures Related to Type of Building or Occupancy

The report gives specified and quantified advice on choice of detector type and on siting arrangements for buildings or occupancies such as health care facilities including hospitals, museums, offices, warehouses, industries.

6.2.2 Reduction of False Alarms from Student Dormitories /41/

False alarm rates from college dormitories were in this report shown to increase the point where alarm credibility was more or less destroyed. Three different kinds of changes in detector system design were introduced.

a. Desensitization of smoke detectors by changing the resistivity of the electric circuit meant increasing the threshold obscuration from 1.5%/ft to 2.5%/ft (optical density changed from 0.22 to 0.38 dB/m, cf the EN54 part 9 specifications). As a consequence false alarms were reduced by more than 60%.

b. The introduction of alarm verification modules decreased false alarm in one dormitory by 75%, in another by 41%. "Alarm verification" meant that the detector was checked again 60 seconds after activating to confirm response consistency before alarm was relayed.

c. "Hardened" smoke detectors with improved resistance to false alarm from entrapped dust reflectivity, insect penetration, humidity, condensation and radio interference reduced false alarm rate by some 50%.

6.2.3 The U.L. Position /48/

Reference 48 contained notes on a presentation at the 1986 National Bureau of Standards Conference on Fire Research by Peter Dubivsky, Underwriters Laboratories. The following is a direct quotation from Fire Technology.

"Peter Dubivsky (Underwriters Laboratories), "False Alarms from Smoke Detectors: A Survey of the Experience of a Major User." This paper summarized a study of smoke detectors in VA hospital facilities. The study was designed to find causes and remedies of false alarms. The next step is analysis of product changes and changes in designs and applications.

A false alarm was defined as a signal resulting from a non-hostile fire or some environmental phenomenon. Results of the survey showed a rate of 0.171 false alarms per detector per year or 16.8 false alarms per real alarm. The goal of the project is to have 1.0 false alarms per real alarm.

The identified causes of false alarms, in order of frequency, were as follows: high senisitivity; smoking; lack of cleaning, accumulation of dust or lint; construction dust; abnormal air velocity (only for ionization units); insects; high humidity; electrical sources, malicious; combinations of factors; misapplications (wrong locations).

The list of remedies for the causes was as follows:

1. High sensitivity:	Test semiannually for sensitivity and replace units that fail. Reduce sensitivity to new UL minimum, coordinating with UL and local authority. Add alarm verification if problem persists.
2. Smoking:	Establish and enforce smoking-area policy. Add alarm verification if problem persists.
3. Lack of cleaning:	Conduct semiannual cleaning policy in concert with testing schedule of NFPA 72E.
4. Construction dust:	(Not recorded by the author)
5. Abnormal air velocity	Switch to photoelectric units or other ionization units that are not affected.
6. Insects:	Use insect repellent.
7. High humidity:	Use a unit acceptable under these conditions.
8. Electrical sources:	Use units that are not affected. Add alarm verification if needed.
9. Other three:	No remedies cited.

Regarding the high sensitivity remedies, Dubivsky stated that the current UL allowed range is 0.5-0.4 obscuration percent per foot, replacing an older range that extended to 0.2. His data, however, showed a marked change in false claim rate for all detector models - and only those detector models - whose obscuration percent rates ranged below 1.0 percent per foot."

Remark: According to the 1976 edition of UL 168 the allowable ranges of detector operation are the following:

		obscuration %/ft	optical density dB/m
gray smoke	max	4.0	0.0581
	min	0.2	0.0033
black smoke	max	10.0	0.151
	min	0.5	0.0072

6.2.4 Some Japanese Data

A substantial part of the extensive Japanese fire research seems to be in the detection area. Unfortunately, most of the research information is published only in Japanese and, for practical purposes, unavailable to foreigners. As an example, the 1985 Annual Conference on Fire Research notes include five presentations linked to the detections problem. However, a useful overview in English is published in /38/. Regarding false alarms, some of the methods and practical results mentioned are

- adoption of alarm verification of the time delay type decreases the false alarms by 45%

- individually adressable detectors with automatic checking of sensitivity gives a system with false alarm occurrence of 0.15%/year and detector.

Statistics show that the overall, averaged probabilities of false alarm per year in Japan with existing systems are 6.5% for smoke detectors and 0.8% for heat detectors. The goal is to reduce the smoke detector figure to 1%. Old systems will be upgraded by the methods mentioned earlier in this chapter. For new systems, software control and application of pattern recognition methods are expected to lead to a greatly improved reliability.

6.2.5 Software Control and the BRESENS System

Very few data are published regarding experiments with software controlled detection systems. The report in /49/ gives results from field tests with Bresens, an "intelligent" automatic fire detection system developed at Fire Research Station, UK. Fire tests were carried out

a) to determine sensor output, changes in the presence of different types of fire

b) to determine the response of BRESENS to different types of fires.

Similarly, a set of "false alarm susceptibility tests" were carried out (temperature, humidity, air pressure, air velocity, tobacco smoke, airborne dust, electrical interference, etc).

The experimental data were transferred to a minicomputer to determine what algorithm should be employed to descriminate between fire and false alarms. Features of the tested algorithms included

a) drift compensation

b) transient filtering (electronic overload, radio interference)

c) checking against "threshold" and "rate of rise" levels.

Evidently the analysis is still going on but some conclusions were reached in /49/. It emerged that a dramatic reduction of false alarm frequency is within reach using the software controlled checking procedures mentioned above. One particular useful feature of the system was the ability to contionuously report how often the varous filtering and monitoring procedures were activated and thus make possible an evaluation of system detoriation. Also, records of pre-alarm, "near misses" situations will assist in diagnosing the system performance. There was no direct indication that more complex, pattern recognition can be usefully employed at the present stage. Analogue sensor signals from fire and non-fire, alarm-causing exposures seem to exhibit similar patterns.

6.3 Tentative Conclusions

* National false alarm statistics imply that the false alarm rate in Sweden is comparable with that of other countries

* introduction of software-controlled system (including drift compensation, filtering of electronic transients, compensation for changes in ambient temperature and aerosol concentration, introduction of alarm verification etc but not explicit aerosol pattern recognition algorithms) should reduce the false alarm rate to the vicinity of the rate of real alarms

* existing systems will remain the big problem

* possible remedies include
  - desensitization (calculations in chapter 8 will illustrate the practical consequences of this measure)
  - a control of existing systems against the siting instructions for example given in /47/. Possibly a review of the present installation standard RUS 110 is in order
  - the introduction of an "alarm organization" in health care facilities, hotels, industrial complexes, etc, see the report in "Brand och Räddning" 4/87 /50/. A vital element is the training of the working force /51/, especially of the technical maintenance staff.

7 ENGINEERING DESIGN METHODS FOR THE SITING OF DETECTORS

7.1 Heat Detectors

Equations in section 3.2 describe gastemperature and gas velocity in the turning region, and ceiling jet region respectively. These are the expressions which determine the detector environment. Equations 5.1 - 5.3 describe the response of the sensing element to an arbitrary ceiling jet gas temperature increase ΔT. The concept of the response time index RTI was introduced in 5.1. Hence, given the RTI, together with ΔT_g and U as functions of time, the thermal response $\Delta T_L(t)$ can be calculated. Detector actuation occurs when $\Delta T_L = \Delta T_{La}$, where ΔT_{La} is the actuation temperature of the heat responsive element above ambient.

Section 7.1 will describe four element of a design process: a method to measure RTI, an explicit solution to Eq 5.1 for fires growing according to t^2, a computational methodology using hand calculations and, finally, the use of a computer program and calculated design tables.

7.1.1 The RTI-Value and the Plunge Test

The various assumptions of the response theory were originally examined in some detail in /52/, with the following conclusions:

"1) Forced convection would indeed be the dominant mode of heat transfer to the heat responsive element in most fire situations relative to both free-convection effects and radiation from the fire;

2) the element would most likely heat in approximate isothermal manner, as assumed, in the sense that temperature differentials within the element would generally be small compared to the average temperature rise of the element from ambient conditions;

3) assuming negligible actuation heat may be questionable for heavily solder-loaded, heat responsive elements, depending on the effective solder fraction which has to be fused before the element actuates;

4) quantitative estimates of conduction heat loss from an element are so difficult that the errors associated with ignoring this loss are not readily assessed."

A special test apparatus, the "plunge test" was developed to determine the necessary RTI-values of the sensing elements of sprinklers and heat detectors /52/. Recently, the constancy of RTI was questioned /53/ for fire situations where gas velocities are low at siting location. The phenomenon was attributed to conductive heat loss from sensing element to

the housing or fitting. In /53/, a theory was developed to include the conductive heat loss from element. The theory requires in additon to the RTI-value a heat conduction parameter C. A methodology to experimentally determine C was described and the influence of C on response time for some RTI-values, fire room geometry and fire growth rates determined. The general result was that conductive heat loss is primarily important at low gas temperatures and velocities. More definite conclusions will require further investigation.

7.1.2 Calculation of Response Times for t^2 - Fires

For fires growing according to t^2

$$\dot{Q} = \alpha\ t^2$$

Beyler /18/ demonstrated that Eq 5.1 has an analytical solution. Using the condition that the initial detector element temperature is equal to ambient temperature ($T_L = T_\infty$), the equations for calculating the response of fixed temperature and rate of temperature rise detectors are, from Beyler;

$$\frac{dT_L}{dt} = \frac{(4/3)\ (\Delta T/\Delta T_2^*)\ (\Delta T_2^*)^{1/4}}{(t/t_2^*)\ (0.188 + 0.313\ r/H)}\ (1 - e^{-Y}) \qquad (7.1)$$

$$T_L - T_L(0) = (\Delta T/\Delta T_2^*)\ \Delta T_2^* \left[1 - \frac{(1 - e^{-Y})}{Y}\right] \qquad (7.2)$$

where

$$Y = \frac{3}{4} \left[\frac{U}{U_2^*}\right]^{1/2} \left[\frac{U_2^*}{\sqrt{\Delta T_2^*}}\right]^{1/2} \frac{\Delta T_2^*}{RTI} \left[\frac{t}{t_2^*}\right] (0.188+0.313r/H)$$

7.1.3 Hand Calculation

In a design situation, the objective is to determine the spacing of detectors required to respond to a specific fire scenario. Design criteria is usually a limit size of the rate of heat release of the fire, alternatively a maximum time to activation. The calculation may follow the following scheme /54/.

1. Determine the environmental conditions of the area being considered. They are; a) T_∞ and b) H.
2. Estimate the fire growth characteristic α
3. Establish the goals of the system: response time, t_r, or threshold fire size at response, Q_T.
4. Select the detector type to be used. For fixed temperature units this establishes the detector response temperature and its RTI.

5. Make a first estimate of the distance, r, from the fire to the detector.
6. Assume that the fire starts obeying the power law model at time t = 0.
7. Set the initial temperature of the detector and its surroundings at ambient temperature.
8. Use Beyler's solution to calculate the resulting temperature of the detector. The equations necessary for this solution is Eq 7.2.
9. If the temperature of the detector is below its operating temperature, this procedure must be repeated using a smaller r. If the temperature of the detector exceeds its operating temperature, a larger r can be used.
10. Repeat this procedure until the detector temperature is about equal to its operating temperature. The required spacing of detectors is then S = 1.41 x r.

7.1.4 Computer Program and Ready-Calculated Design Tables

To minimize work, it is recommended that the computer program DETACT-T2, described and listed in /55/ and /56/ is used. Still more convenient is the use of the extensive design tables listed in /56/. Time to actuation has been calculated for the following range of design parameters

fire growth process: α = 0.00293, 0.0117, 0.0469 and 0.1875 kW/s^2

ceiling height: 1 - 24 m

RTI: 0 - 400 (m · s)$^{1/2}$

actuation temperature rise: 5 - 80°C

For rate of rise detectors, values of 8, 10 and 14°C/min have been used.

Application Example

A single example will demonstrate the practical consequences of the present siting rules. The table below gives time to actuation and corresponding fire sizes (values in kW within parenthesis) for a heat detector with RTI = 50 (ms)$^{1/2}$, exposed to the four standard fire growth processes and in buildings of different ceiling heights H.

TABLE 7.1 Time for actuation for heat detectors, exposed to four standard fire growth processes and in buildings of various height H.

Type of fire	Height H of ceiling (m)				
	4	7	10	12	18
Ultrafast α=0.1875 kW/s^2	2.46 min (4086)	2.89 min (5638)	3.36 min (7620)	3.69 min (9190)	4.73 min (15101)
Fast α=0.0469 kW/s^2	3.89 min (2554)	4.72 min (3761)	5.63 min (5351)	6.27 min (6637)	8.28 min (11575)
Medium α=0.0117 kW/s^2	6.45 min (1752)	8.14 min (2790)	9.95 min (4170)	11.19 min (5180)	15.10 (9603)
Slow A=0.0029 kW/s^2	11.27 min (1326)	14.72 min (2262)	18.30 min (3496)	20.75 min (4495)	28.38 (8407)

For the range of parameters chosen, actuation time will vary between 2.46 and 28.38 minutes and fire size at detection from 1326 kW to 15101 kW

7.2 Smoke Detectors

7.2.1 Temperature Rise Versus Optical Density at Actuation

The description of the detector environment required for designing the siting of smoke detectors is far more complex than that required for heat detector. As discussed earlier the "sensitivity" of a smoke detector can be seen as a function of two factors: the material that is being burnt and the inherent characteristics of the detector itself. The investigations in /16/ produced the useful finding that optical densities, measured with a specified photometer at a certain location and for a given combustible material, are in an approximately constant ratio to the measured local temperature rise.

Table 7.2 gives examples on measured $D_L/\Delta T$-values /16/.

TABLE 7.2 Measured values of the ratio $D_L/\Delta T$, where D_L denotes optical density and ΔT temperature rise /16/

Material	$D_L/\Delta T$ (ob/^oC)
Wool	0.012
Cotton fabric	0.006/0.012
Paperwaste basket	0.018
PU foam	0.24
Polyester fiber	0.18
PVC insulation	0.3/0.6
Foam rubber	0.78

Roughly, the ratio varies within the bracket 100:1 for the materials investigated. The constancy for a given material can be explained theoretically if

- smoke production measured in mass units is proportional to convective heat release

- coagulation effects in plume and ceiling jet flow are unimportant

- heat transfer from ceiling jet flow to the ceiling material may be neglected.

The values in Table 7.2 are approximate averages. Deviations from the requirements above meant that $D_L/\Delta T$-values for a given combustible varied with time at a specific measurement point and with measurement location for a specified time after ignition. For the individual fuel, there was an approximate 10:1 variation in the $D_L/\Delta T$-value. Consequently, these variations, although substantial, are much smaller than the observed difference between different fuels. It was also observed that response of the smoke detector for a given material occurred at a fairly constant level of optical density, independent of location. The variation from one detector to another and between various fuel sources are illustrated in the following table /16/, which alse shows temperature rise ΔT at actuation.

TABLE 7.3 Values of optical density and local temperature rise at time of actuation for two detectors of the ionization type (ID) and photoelectric light scattering type (PSD)

	ID		PSD	
Fire source	optical density (ob)	ΔT(K)	optical density (ob)	ΔT(K)
Wood cribs	0.16	14.0	0.5	41.7
PU foam	1.63	7.2	1.63	7.2
Cotton fabric	0.02	1.7	0.27	27.8
PVC	3.3	7.2	3.3	7.2

7.2.2 The DMR- and L-values /1/

As illustrated in the table above, any given detector may be very sensitive to the burning of one material and quite insensitive to the burning of another material, since the particle concentration and particle size distribution produced by a given burning rate is a function of the chemistry of the material and its environment. The material response is reflected in the sensitivity designation of the detector, the DMR.

The Fire Detection Institute has presented design curves for detectors with detector sensivities DMR 1, DMR 2 and DMR 3, where DMR 1, 2 and 3 represent specific detector material response numbers (DMR) for a given detector material combination. These are classified on the basis of:

DMR numbers

(Temperature Rise to Detection, ^{o}F)

DMR 1 ≤ 20
DMR 2 21 - 40
DMR 3 41 - 80

DMR values greater than 80 are not given since there is an assumption that detector material response values greater than 80 are inadequate and should not be acceptable.

Having defined the sensitivity of a smoke detector in terms of the DMR numbers, there is a further complication. The DMR numbers are not sufficient when there is resistance to entry of smoke into the detector chamber, which is practically always the case. This resistance to smoke entry may vary considerably from one detector model to the next, even if they have the same DMR numbers for a material. It can be shown that the effect of resistance to smoke entry can be accounted for in terms of the "characteristic length" L of a

detector model. The characteristic length depends only on the detector geometry and can be measured in "smoke boxes" of the kind used by approval laboratories. Unfortunately, the L values of approved smoke detectors are not listed, but they could be if approval laboratories or detector manufacturers decide to measure them.

The report from the Fire Detection Institute further states that L values among approved smoke detectors vary from less than 10 ft to more than 80 ft. The smaller the L value, the less the resistance to smoke entry. The value L = 0 means that there is no resistance to smoke entry. For each of the three selected DMR numbers, the design curves were prepared for five different values of L: 0.5 ft, 10 ft, 20 ft, 40 ft and 80 ft. An example is shown in fig 7.1.

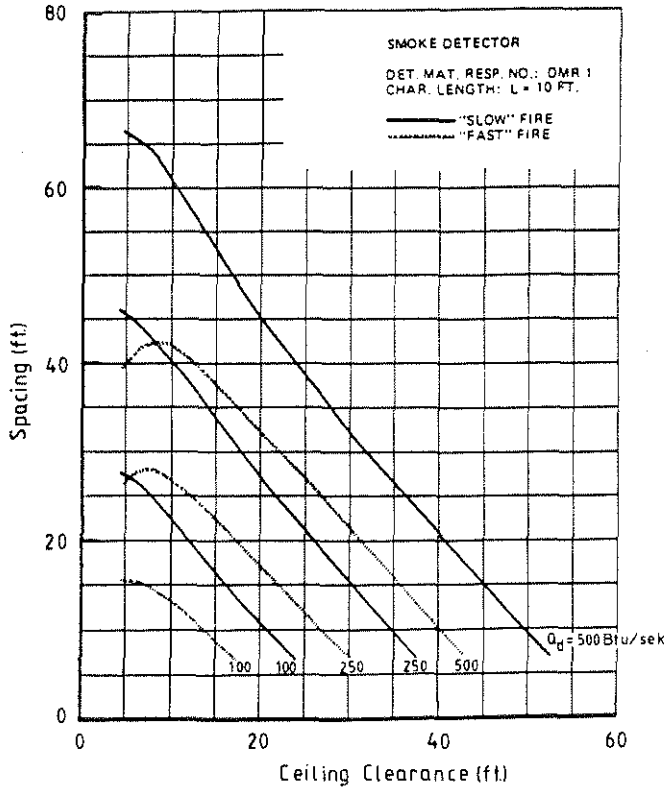

Fig 7.1 Examples of the design curves calculated by the Fire Detection Institute /11/. The curves show the required spacing for the detectors to actuate at fire sizes Q_d = 100 - 500 BTU/sec (≈ 100 - 500 kW) for different ceiling heights

On the problem of not knowing what kind of combustible is involved in the first stage of the fire, the report says:

"Whereas with the heat detector a knowledge of the type of material that might be burning was not needed for determining the detector sensitivity, for the smoke detectors one must know the materials that will be burning in order to determine the sensitivity, and the DMR number for the detector that is

being considered. One alternate for the case where the burning material is not known or readily predictable, may be to take the conservative approach of assuming a wood crib is the burning material. In this case the DMR value will be conservative, a higher value than for the other common materials and would put the detector sensitivity in the DMR 3 classification, except for the most sensitive detectors. This value can then be used with the "L" value of the detector to determine the required spacing."

8 SPECIFIC PROBLEMS

Chapter 8 will, by using some very simplified calculation procedures, illustrate two important problems. The first one concerns the influence on life safety of desensitization of smoke detectors. The second one the effect of aerosol coagulation on detector output.

8.1 The Influence on Lifesafety of Decreasing Detector Sensitivity. Some Calculation Examples

As discussed in chapter 6, a possible method of decreasing false alarm rates is to decrease detector sensitivity. Two specific scenarios have been considered, one involving flaming and one smouldering combustion of a polyurethane mattress in a patient room in a health care facility. The following data apply to the room: room height H = 4.5 m, floor area = 60 m^2, room volume V = 270 m^3. Siting of the detector corresponds to a spacing of 7.5 m.

8.1.1 Flaming Combustion

The mattress will be chosen from the full scale tests carried out within the Brandforsk project "The pre-flashover fire". Test No 3 in /57/ exhibits results where the rate of heat release curve follows

$$\dot{Q} = \alpha\, t^2 \qquad (8.1)$$

with α = 0.003 kW/s^2, which is very close to the α value characterizing the "slow" fire in /56/ (α = 0.00293 kW/s^2). We are thus able to directly use the siting calculation made in /56/. According to Table 7.2, for flaming flexible polyurethane fires

$$\frac{D_L}{\Delta T} = 0.24\ dB/m^oC \qquad (8.2)$$

The assumption is now that we want to investigate the height of the smoke layer at time of evacuation with the detector having two different sensitivities: 0.5 dB/m and 2.0 dB/m, corresponding to the limits m_1 and m_3 described in EN54 part 9. Using Eq 8.2 above, the corresponding temperature increases are $\Delta T_1 \approx 2^oC$, $\Delta T_3 \approx 10^oC$. The actuation times taken from /56/ will be 80 s and 210 s respectively. We now further make the assumption that evacuation starts respectively 0,1 and 2 minutes after detector actuation and calculate /58/ the smoke filling. Assuming that the burning bed is 0.5 m from the floor we arrive at the following vertical distance z from bed

to smoke layer (z in m) just when evacuation starts. m_1 denotes an alarm level of 0.5 dB/m, m_3 a level of 2.0 dB/m, see Table 8.1.

TABLE 8.1 Distance patient bed - smoke layer the moment evacuation starts. Delay time from alarm to start of evacuation is chosen = 0, 1 and 2 minutes and detector sensitivity is chosen = 0.5 and 2.0 dB/m

Time used to start evacuation after alarm has sounded	Smoke density at actuation	Distance Z smoke layer - patient bed at start of evacuation
2 min	m_1=0.5 dB/m	1.16 m
	m_3=2.0 dB/m	0.51 m
1 min	m_1=0.5 dB/m	2.2 m
	m_3=2.0 dB/m	0.72 m
0 min	m_1=0.5 dB/m	2.7 m
	m_3=2.0 dB/m	1.05 m

The figures indicate that decreasing detector sensitivity may increase life hazard dramatically.

8.1.2 Smouldering Fire

We assume a smouldering fire where the fire is so weak that stratification can be ignored and the combustion products uniformly mixed in the room volume V. The task is now to calculate time to CO-intoxication for the hospital patient compared to actuation time for the detector. Following the data in /19/ we take mass smouldering rate $\dot{m}$

$$\dot{m} = ct \text{ g/min}$$

with c = 0.206 g/min^2 and mass generation rate of CO

$$\dot{m}_{co} = \gamma \dot{m}$$

with $\gamma = 0.10$.

According to /59/, the smoke potential of smouldering polyurethane D_o = 5.1 ob * m^3/g. This gives an optical density D_L in the room

$$D_L = 5.1 * \frac{m}{V} \text{ dB/m}$$

where m is total mass loss rate, obtained by integrating Eq for $\dot{m}$ above. It was estimated in /59/ that the critical dose D for CO incapacition is

$$D = 4.5\% * \text{min}$$

Elementary calculation shows that D is given by the relation

$$D = c\gamma t^3/(6\rho V)$$

where ρ = density of gas.

Applying our data gives a critical inhalation time

$$t_{cr} = \left[\frac{6D\rho V}{c\gamma}\right]^{1/3} = \left[\frac{6 * 0.045 * 270}{0.206 * 0.1}\right]^{1/3} = 16 \text{ min}$$

After 16 min total mass loss m = 26.4 g PUR corresponding to an optical density

$$D_L = 0.50 \text{ dB/m}$$

which by coincidence is equal to the m_1 value prescribed in EN54 part 9. For this special case, desensitization seems not to be without risks.

8.2 Smoke Aerosol Coagulation and Detector Sensitivity

To obtain at least a qualitative understanding of the coagulation effect, the detector sensitivity curves from Bukowski and Mulholland, se Fig 5.8, were combined with the aerosol size distributions calculated in /37/. The distributions for t = 0 and 3.0 seconds are shown in Fig 8.1 for the EN54 part 9 test fire with flaming wood earlier shown in Fig 2.1.

As shown in Fig 8.1, the small sizes are rapidly depleted and with relatively small changes in the distribution above 0.05 μ m. At the end of the calculation period, only about 3 percent of the original total number of particles remained. Integrating Figs 5.8 and 8.1, the results were the following

- the output in μV decreased by a factor 50-100 for the ionization type detector R-2

- output for the light-scattering type detector S-2 remained virtually the same.

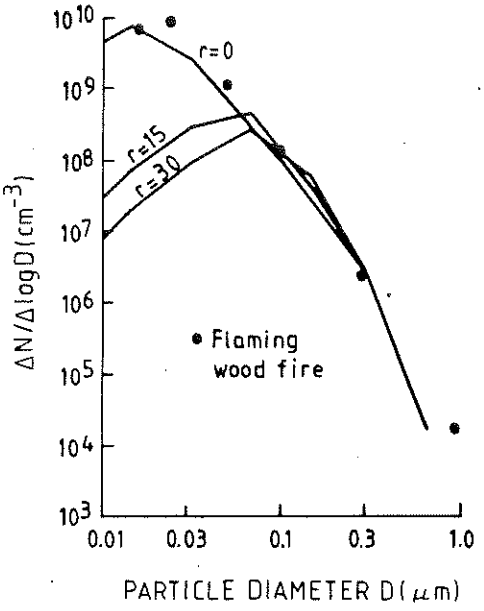

Fig 8.1 Calculated smoke aerosol size distributions showing the evolution of the distribution under the influence of coagulation. The experimental points are taken from Fig 2.1 /21/. r denotes non-dimensional time and r = 30 corresponds to t = 3 sec.

The conclusion is that the coagulation effects in detector output are wholly dependent on initial size distribution and the individual detector sensitivity. The results indicate that ionization detectors may be very sensitive to the ageing effects.

9 SUMMARY

1. The survey has mainly concentrated on the following items: the false alarm problem, the problem of the fire not being detected due to the fact that pre-fire heating and ventilation dominate flow inside the compartment, a description of detector sensitivity to fire signatures, engineering design methods for the siting of detectors.

2. The statistical as well as practical experience suggests that alarm systems in Sweden, follow international trends regarding rates of false alarms.

3. For existing systems, especially the older ones, introduction of a proper alarm organisation, regular training of the technical maintenance staff and/or desensitization may be appropriate measures to reduce the false alarm rate.

4. Analysis shows that desensitization of existing systems must be done with care so life hazard is still kept under control.

5. In addition to the remedies mentioned under point 3 it might be effective to revise the siting standard rules in RUS 110 in the light of the information obtained for example in the Norwegian investigation.

6. A revision of RUS 110 should also be based on scaled down physical modelling and the use of numerical modelling (field modelling) in order to investigate local flow field characteristics: the influence of beamed ceilings, ventilation in- and outflow, a thermally stratified pre-fire atmosphere, etc.

7. In order to take consideration of various fire developments rates and varying ceiling heights, standard siting distance should be calculated according to the design model described in NFPA 72E Appendix C for heat detectors.

8. For smoke detectors, a more rational use of the information obtained in the EN54/9 sensitivity test standard fires should be investigated.

9. Point 3 mentioned existing systems. For new and future systems the gradual improvement in software control (alarm verification procedures, automatic compensation for regular variation in ambient conditions, automatic change of sensitivity to compensate for the gradual accumulation of dust and dirt, filtering of electronic signal spikes, checking of electric circuit integrity etc) is thought to dramatically reduce false alarm rates.

10. Efficient pattern-recognition algorithms for separating fire process environments from the aerosols produced by welding, trucks exhaust, smoking etc may be hard to produce; the aerosol characteristics are too much alike. Algorithms based

on use of data from a group of sensors ("group decision") should be more reliable but may be too complex. In theory, if sensor response to monodisperse aerosols is known and with standard test fire aerosol characteristics experimentally measured, sensor output during the standard test fires should be easily calculable and a first check obtained on the discrimatory capability of pattern recognition algorithms. No information of this kind has been found.

REFERENCES

1 Benjamin, I., Detector Response in Large Buildings, Proceedings Engineering Application of Fire Technology Workshop April 16-18 1980, NBS, Gaithersburg

2 Lee, T.G.K. and Mulholland, G., Physical Properties of Smoke Pertinent to Smoke Detector Technology, NBSIR 77-1312, NBS Nov 1977

3 Helsper, C. and Fissan, H.J., Particle Number Distributions of Aerosols from Test Fires, Journal of Aerosol Science, Vol 11 439-446 1980

4 Seader, J.D. and Einhorn, I.N., Some Physical, Chemical, Toxicological and Physiological Aspects of Fire Smokes, 16 Symp. (Int.) on Combustion, The Combustion Institute, pp 1423, 1977

5 Rasbash, D.J. and Pratt, B.T., Estimation of the Smoke Produced in Fires, Fire Safety Journal, Vol 2, 23-37, 1979/1980

6 Olander, Ventilation, Studentlitteratur 1982

7 Johansson, G.I. et al, A Study of Indoor Aerosol Distribution and Attachment of Radon Daughters, Journal of Aerosol Science, Vol 14, 455-458, 1983

8 Alpert, R.L., Fire Induced Turbulent Ceiling Jet, Factory Mutual Research Report, FMRC Serial No 19722-2, May 1971, p 74

9 Stroup, D., Evans, D. and Martin, P., Evaluating Thermal Fire Detection Systems (SI Units) National Bureau of Standards Special Publication 713, April 1986

10 Burry, P. (Personal communication)

11 Cox, G., Kumar, S. and Markatos, N.C., Some Field Model Validation Studies, The 1st International Symposium on Fire Safety Science, Hemisphere Publishing Corp. 1986, p 159

12 Handa, T., Morita, M. et al., Computer Simulation of the Motion of Heat Flow Induced by the Fire in the Longscale Tunnel, Fire Service and Technology, Vol 1, 1981, p 91

13 Yamauchi, Y., Numerical Simulations of Smoke Movement and Coagulation, The 1st International Symposium on Fire Safety Science, Hemisphere Publishing Corp 1986, p 719

14 Johnson, P.F., Fire Detection in Computer Facilities, Fire Technology 22(1) 1986, p 14

15 Alpert, R.L., Calculation of Response Time of Ceiling - Mounted Fire Detectors, Fire Technology, 8, 1972, p 181

16 Heskestad, G. and Delichatsios, M.A., Environments of Fire Detectors Phase I; Effects of Fire Size, Ceiling Height and Material, Volume II - analysis, Technical Report Serial No. 22427, RC 77-T-11, Factory Mutual Research Corporation, Norwood, Massachusetts 02062, 1977

17 Heskestad, G. and Delichatsios, M.A., The Initial Convective Flow in Fire", Seventeenth Symposium (International) on Combustion, The Combustion Institute - Pittsburgh, Pennsylvania, 1978, pp. 1113-1123

18 Beyler, C.L., A Design Method for Flaming Fire Detection, Fire Technology, 20, 4, 1984, p 5

19 Quintiere, J. et al, An Analysis of Smouldering Fires in Closed Compartments and Their Hazards Due to Carbon Monoxide, National Bureau of Standards NBSIR 82-2556, July 1982

20 Heskestad, G. and Smith, H.F., Investigation of a New Sprinkler Sensitivity Approval Test: The Plunge Test, Technical Report Serial No. 22485 RC 76-T-50, Factory Mutual Research Corporation, Norwood, M.A. 02062, 1976

21 Evans, D.D., Calculating sprinkler Actuation Time in compartments. Fire Safety Journal 9, (1985) 145-155

22 Heskestad, G., The sprinkler Response Time Index (RTI). Paper (RC81-TP-3) presented at the Technical Conference on Residential Sprinkler Systems, FMRC, Norwood, MA, April 28-29, 1981

23 Luck, H.O. and Deffte, N., Dynamic performance of pneumatic tube type heat sensitive fire detectors, Fire Safety Science, Proc. 1:st Int. Symp 1985, 729

24 Unokiand J. and Kimura, S., New fire detector for road tunnels. AUBE'82 Probleme der automatischen Brandentdeckung, 1982, 134

25 Barrett, R. and Middleton, J.F., Optimum design of infra-red flame detectors. BRE Symposium No 6 Automatic fire detection. Proceedings of the Symposium held at the Connaught Rooms, London 8-10 March 1972, 116

26 Middleton, J.F. and Eng, C., Developments in Flame Detectors, AUBE'82. Probleme der automatischen Brandentdeckung 1982, 119

27 Heitmann, H., Ein Beitrag zum Entwurf und Test von Ultraviolett-Flammenstrahlungs-Meldern fur die automatische Brandentdeckung AUBE'82. Probleme der automatischen Brandentdeckung 1982, 182

28 Stevens, J.R., Ultraviolet radiation detector for aircraft engines. BRE Symposium No 6, Automatic fire detection. Proceedings of the Symposium held at the Connaught Rooms, London 8-10 March 1972, 126

29 Holker, J.R. and Lomax, G.R., Sensory early warning systems in fire detection. "New Technology to reduce Fire Losses and Costs" ed S.J. Grayson and D.A. Smith, Elsevier Applied Sciences Publishers, 1986, pp 248

30 Pfister, G., Detektion von Brandgasen mit Festkörpersensoren Schwerpunkte der Forschungsaktivität. ABE'82 Probleme der automatischen Brandentdeckung, 1982, 106

31 Bukowski, R.W. and Mulholland, G.W., Smoke Detector Design and Smoke Properties, NBS Technical Note 973, 1978

32 DiNenno, P.J. and Dungan, K.W., Effectiveness of Fire-Detection Systems in Light-Water-Reactor Facilities, ALO-141. Sponsored by U.S. Dept of Energy Saudia Contract No 49-1716, Aug 1981

33 Hosemann, J.P., Veber verfahren zur Bestimmung der korngrossenverteilung hochkonzentrierter Polydispersionen von die elektrischen Mie-Partikeln, Dissertation T H Aachen (1970)

34 Scheidweiler, A., Physical aspects of ionization chamber measuring techniques (unipolar and bipolar chambers), Fire Detection for Life Safety, Proceedings of a symposium National Academy of Sciences (1977)

35 Avlund, M., Reference Measurements of Smoke Density, ECR-71, May 1977

36 Brand & Räddning 6-7/87 p 44 "I Göteborg har man misslyckats totalt"

37 Baum, H.R., Rehm, R.G. and Mulholland, G.W., Prediction of Heat and Smoke Movements in Enclosure Fires, Fire Safety Journal, Vol 6, 1983, p 193-201

38 Watanabe, A., Sasaki, H. and Unoki, J., The 1st International Symposium on Fire Safety Science, Hemisphere Publishing corp, 1986 p 679

39 Fry, J.F., "Über Probleme der automatischen Brandentdeckung". Tagungsbericht des 6. international Vortragseminar (1971). Institute für Elektrischen Nachtrichenteknik der RWTH, Aachen West Germany

40 Fry, J.F. and Eveleigh, C., Fire Protection Association Journal, Oct 1970

41 Breen, D.E., Improved Life Safety through more reliable smoke detector systems. "New Technology to reduce Fire Losses and Costs", ed S.J. Grayson and D.A. Smith, Elsevier Applied Science Publishers Ltd 1986, pp 229

42 Burry, P.E., Current Research on Fire Detection at the Fire Research Station, CP 38/75

43 Luck, H.O., Correlation Filters for Automatic Fire Detection Systems, Proc 1:st Int Symp on Fire Safety Science, 1985, 749

44 Harwood, J. and Hume, B., The Application of Microprocessors to Automatic Fire Detection Systems "New Technology to reduce Fire Losses and Costs", Ed Grayson, S.J. and Smith, D.A. Elsevier Applied Science Publishers, 1986, 235

45 Maillet, M., Microprocessors and New Communication Systems in Improved Detection Systems, "New Technology to reduce Fire Losses and Costs", Ed Grayson, S.J. and Smith, D.A. Elsevier Applied Science Publishers, 1986, 243

46 Johnson, P.F., Letter to the Editor, Fire Technology 22(4) 1986, p 352

47 Jensen, G., Falske alarmer, Delrapport 4 Brannsikring - Spesielt med Tanke på Brannalarmanlegg, Elektroniklab NTH, Trondheim, Mars 1983

48 Fire Technology May 1987

49 Harwood, J. and Hume, B., The Application of Microprocessors To Automatic Fire Detection Systems, Same volume as ref 45, p 235

50 Bergstrand, G. and Landström, L.H., Bot Mot Falsklarm, Brand & Räddning 4/87 p 15

51 Brand & Räddning 12/86 p 55

52 Heskestad, G. and Smith, H.F., Plunge Test for Determination of Sprinkler Sensitivity, FMRC 3A1E2.RR FMRC, Norwood, Mass., Dec 1980

53 Heskestad, G. and Bill, R.G., Quantification of Thermal Responsiveness of Automatic Sprinklers - RTI, etc SFPE Symposium on Fire Detection and Suppression, Linthicum Heights, Md, March 9-11, 1987

54 Schifiliti, R.P., Engineering Fire Detector and Sprinkler Response, SFPE Bulletin, April 1987

55 Evans, D.D. and Stroup, D.W., Methods to Calculate the Response Time of Heat and Smoke Detectors Installed Below Large Unobstructed Ceilings, BSIR 85-3167, July 1985

56 Stroup, D., Evans, D. and Martin, P., Evaluating Thermal Fire Detection Systems (SI Units), NBS Special Publication 713, April 1986

57 Andersson, B., Fire Behaviour of Beds and Upholstered Furniture - An Experimental Study (Second Test Series), Lund Institute of Technology, Divison of Building Fire Safety and Technology, Report LUTVDG/(TVBB-3023) 1985

58 Tanaka, T. and Yamana, T., Smoke Control in Large Spaces, Fire Science and Technology, Vol 5, No 1 1985 pp 31-40

59 Rasbash, D.J. and Philips, R.P., Quantification of Smoke Produced at Fires, Fire and Materials, Vol 2, No 3 1978